Acta Cryst C STRUCTURAL CHEMISTRY
ISSN 2053-2296

Structure determination and Hirshfeld surface analysis of new cocrystal and salt forms of 5-aminotetrazole with hydroxy- and nitro-substituted carboxylic acids

Jeyaraman Selvaraj Nirmal Ram,[a]* Udhayasuriyan Sathya,[a] Sundaramoorthy Gomathi[b] and David Bradford Cordes[c]

[a]Centre for Research and Development, PRIST Deemed to be University, Thanjavur 613 403, Tamil Nadu, India, [b]Department of Chemistry, Periyar Maniammai Institute of Science and Technology, Thanjavur 613 403, Tamil Nadu, India, and [c]School of Chemistry, University of St Andrews, North Haugh, St Andrews, Fife, KY16 9ST, United Kingdom. *Correspondence e-mail: nirmalramjs@gmail.com

Received 19 April 2022
Accepted 23 June 2022

Edited by M. Rosales-Hoz, Cinvestav, Mexico

Keywords: 5-aminotetrazole; intermolecular interaction; crystal structure; comparative analysis; Hirshfeld surface analysis; two-dimensional fingerprint plot.

CCDC references: 2181468; 2181467

Supporting information: this article has supporting information at journals.iucr.org/c

Two new crystalline solids, namely, 5-aminotetrazole–3,5-dihydroxybenzoic acid–water (1/4/6), $CH_3N_5{\cdot}4C_7H_6O_4{\cdot}6H_2O$ (**I**), and 5-aminotetrazolium 3,5-dinitrosalicylate, $CH_4N_5^+{\cdot}C_7H_3N_2O_7^-$ (**II**), have been synthesized and characterized by single-crystal X-ray diffraction and Hirshfeld surface analysis. The crystal packing arrangements of **I** and **II** are governed by N—H···O and O—H···O hydrogen-bonding interactions. In cocrystal **I**, adjacent acid molecules are linked through O—H···O hydrogen bonds, forming a dimer with an $R_2^2(8)$ motif. In salt **II**, the tetrazolium cation and acid anion are linked through N—H···O hydrogen bonds to also form a dimer with an $R_2^2(8)$ motif. Further N—H···O and O—H···O hydrogen bonds help to stabilize the crystal packing, along with aromatic π–π stacking interactions in **I** and carbonyl···π interactions in **II**. The Hirshfeld surface analysis and fingerprint plots reveal that O···H/H···O interactions contribute 34.4% of the total interactions in the crystal packing of cocrystal **I** and 36.7% in salt **II**.

1. Introduction

5-Aminotetrazole (**AT**), a five-membered heterocyclic tetrazole derivative, is 80% by mass N atoms. The five N atoms present make it a potential building block for constructing metal–organic frameworks (MOFs) and other coordination complexes (Yang *et al.*, 2012; Fujihisa *et al.*, 2011; Neochoritis *et al.*, 2019; Kiselev & Gritsan, 2009). The amphiprotic nature of **AT** allows it to act as either an anion or a cation in a multicomponent reaction medium (Albert *et al.*, 1948; Boraei, 2001). Over the past few decades, interest in the study of tetrazole derivatives has increased rapidly because of its extensive application in the fields of medicine, biochemistry, materials science (industrial materials), coordination chemistry and organometallic chemistry (Torii *et al.*, 2004; Aromi *et al.*, 2011). Tetrazole derivatives have shown anti-inflammatory, anti-arthritic, analgesic and coccidiostat properties (Singh *et al.*, 1980; Bradbury *et al.*, 1993; Upadhayaya *et al.*, 2004), and among these derivatives, **AT** is a multidentate organic ligand that does not have a genotoxicity effect in mammals. As with perchlorate, AT inhibits the sodium iodide symporter and reduces the transport of iodine from moving into the thyroid follicular cells (Adams *et al.*, 2020). **AT** and its salts are also used extensively in pyrotechnics because of the attractive colours they emit and their environmentally friendly nature (Budevich *et al.*, 2021). **AT** exists either in the amino or imino

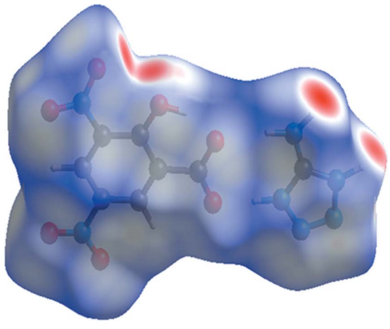

Table 1
Experimental details.

For both structures: $Z = 4$. Experiments were carried out at 173 K. Absorption was corrected for by multi-scan methods (*CrysAlis PRO*; Rigaku OD, 2019). H atoms were treated by a mixture of independent and constrained refinement.

	I	**II**
Crystal data		
Chemical formula	$CH_3N_5{\cdot}4C_7H_6O_4{\cdot}6H_2O$	$CH_4N_5^+{\cdot}C_7H_3N_2O_7^-$
M_r	809.65	313.21
Crystal system, space group	Monoclinic, *Cc*	Monoclinic, $P2_1/c$
a, *b*, *c* (Å)	9.4539 (6), 29.9892 (15), 13.1934 (10)	6.2591 (3), 11.1312 (5), 17.2257 (9)
β (°)	106.454 (7)	98.646 (5)
V (Å^3)	3587.3 (4)	1186.50 (10)
Radiation type	Mo $K\alpha$	Cu $K\alpha$
μ (mm^{-1})	0.13	1.37
Crystal size (mm)	0.21 × 0.14 × 0.04	0.07 × 0.03 × 0.01
Data collection		
Diffractometer	Rigaku SCXMini	Rigaku XtaLAB P100K
T_{min}, T_{max}	0.993, 1.000	0.860, 1.000
No. of measured, independent and observed [$I > 2\sigma(I)$] reflections	22166, 11003, 5256	4182, 4182, 3644
R_{int}	0.060	0.041
(sin $\theta/\lambda)_{max}$ (Å^{-1})	0.740	0.603
Refinement		
$R[F^2 > 2\sigma(F^2)]$, $wR(F^2)$, S	0.066, 0.152, 0.98	0.041, 0.114, 1.04
No. of reflections	11003	4182
No. of parameters	601	221
No. of restraints	30	6
$\Delta\rho_{max}$, $\Delta\rho_{min}$ (e Å^{-3})	0.37, −0.28	0.46, −0.43
Absolute structure	Flack x determined using 1769 quotients $[(I^+) - (I^-)]/[(I^+) + (I^-)]$ (Parsons *et al.*, 2013)	–
Absolute structure parameter	0.4 (7)	–

Computer programs: *CrystalClear-SM Expert* (Rigaku, 2015), *CrysAlis PRO* (Rigaku OD, 2019), *SHELXT2018* (Sheldrick, 2015*a*), *SHELXL2018* (Sheldrick, 2015*b*), *Mercury* (Macrae *et al.*, 2020), *PLATON* (Spek, 2020), *POVRay* (Cason, 2004) and *enCIFer* (Allen *et al.*, 2004).

tautomeric form (Scheme 1), The imino form (**a** in Scheme 1) is more predominant in the solid state (Katritzky & Lagowski, 1963; Butler, 1977; Zhang *et al.*, 2009; Levchik *et al.*, 1992). But in the crystalline state, be it a salt or cocrystal, so far the AT molecule always displays the amine tautomeric form (**b** in Scheme 1).

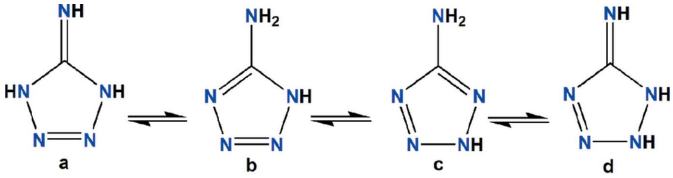

Scheme 1

The crystal structure of **AT** has been reported in the monohydrate form (Britts & Karle, 1967; Bray & White, 1979) and as the picrate (Jin *et al.*, 2005), perchlorate (Klapötke *et al.*, 2008), sulfate (Sinditskii *et al.*, 1995) and halogenide (von Denffer *et al.*, 2008) salts. The structures of several metal complexes (Li *et al.*, 2008, 2019; Ernst *et al.*, 2007) are also known. Different solid forms of **AT** have been used in pharmaceutics and pyrotechnics. Because of its application in many fields and since a very limited number of solid forms of **AT** have been reported so far, we have synthesized two new solid forms of **AT**. Generally, excipients containing carboxylic acid groups are used for the formation of salts and cocrystals (Mishra & Pallepogu, 2018). We report herein the crystal structures of 5-aminotetrazole–3,5-dihydroxybenzoic acid–water (1/4/6), **I**, and 5-aminotetrazolium 3,5-dinitrosalicylate, **II** (see Scheme 2).

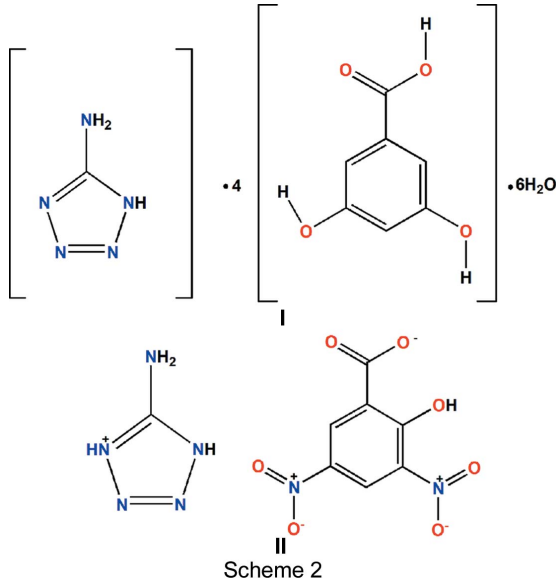

Scheme 2

Dihydroxybenzoic acid (**DB**) derivatives are well known for their biological applications. Compounds like 2,3-dihydroxybenzoic acid, 3,4-dihydroxybenzoic acid and 2,5-dihydroxybenzoic acid have antioxidant properties (Kawase *et al.*, 1988;

Table 2
Hydrogen-bond geometry (Å, °) for **I**.

D—H···A	D—H	H···A	D···A	D—H···A
O1A—H1A···O2B^{i}	0.99 (3)	1.64 (3)	2.617 (5)	168 (6)
O1B—H1B···O2A^{ii}	0.98 (3)	1.65 (3)	2.626 (5)	177 (7)
O1C—H1C···O2D^{ii}	0.98 (3)	1.68 (3)	2.631 (5)	163 (5)
O1D—H1D···O2C^{i}	0.96 (3)	1.69 (3)	2.630 (5)	165 (5)
O1W—H1WA···O6W	0.96 (3)	1.94 (3)	2.899 (5)	179 (5)
O1W—H1WB···O4B^{iii}	0.95 (3)	1.98 (3)	2.920 (5)	167 (5)
O2W—H2WA···O3A	0.95 (3)	1.93 (3)	2.865 (5)	166 (5)
O2W—H2WB···O4D	0.97 (3)	1.92 (3)	2.843 (5)	158 (5)
O3A—H3A···O3B	0.99 (3)	1.76 (3)	2.743 (5)	172 (7)
O3B—H3B···O1W	0.96 (3)	1.70 (3)	2.657 (5)	170 (6)
O3C—H3C···O3D^{iv}	0.95 (3)	1.80 (3)	2.750 (4)	175 (5)
O3D—H3D···O3W^{iii}	0.95 (3)	1.64 (3)	2.582 (5)	168 (6)
O3W—H3WA···N3	0.97 (3)	2.68 (3)	3.610 (6)	161 (6)
O3W—H3WA···N4	0.97 (3)	1.85 (3)	2.784 (6)	162 (6)
O3W—H3WB···O4B^{v}	0.95 (3)	2.21 (5)	2.998 (6)	140 (5)
O3W—H3WB···O4D	0.95 (3)	2.37 (6)	2.942 (5)	119 (5)
O4A—H4A···O2W^{iii}	0.95 (3)	1.76 (3)	2.690 (5)	166 (6)
O4B—H4B···O4A^{iv}	0.98 (3)	1.74 (3)	2.701 (5)	165 (6)
O4C—H4C···O5W	0.95 (3)	1.71 (3)	2.607 (5)	154 (5)
O4D—H4D···O4C	0.93 (2)	1.75 (3)	2.672 (4)	169 (4)
O4W—H4WA···N2^{vi}	0.97 (3)	2.01 (4)	2.918 (6)	156 (5)
O4W—H4WB···O2A^{v}	0.94 (3)	2.04 (3)	2.936 (6)	158 (5)
O5W—H5WA···O4W	0.96 (3)	1.85 (3)	2.773 (5)	162 (6)
O5W—H5WB···O3C^{iii}	0.95 (3)	1.95 (3)	2.901 (5)	172 (6)
O6W—H6WA···N3^{vii}	0.96 (3)	1.97 (3)	2.885 (6)	159 (5)
O6W—H6WB···O2D^{viii}	0.96 (3)	1.95 (3)	2.876 (5)	161 (5)
N1—H1···O6W^{ix}	0.98 (3)	1.86 (3)	2.837 (6)	172 (5)
N6—H6E···O2W	0.95 (3)	2.11 (3)	3.065 (5)	177 (6)
N6—H6F···O4W^{viii}	0.96 (3)	2.07 (3)	2.973 (7)	157 (5)

Symmetry codes: (i) $x+\frac{1}{2}, y+\frac{1}{2}, z$; (ii) $x-\frac{1}{2}, y-\frac{1}{2}, z$; (iii) $x+1, y, z$; (iv) $x-1, y, z$; (v) $x, -y+1, z-\frac{1}{2}$; (vi) $x+\frac{1}{2}, y-\frac{1}{2}, z$; (vii) $x+1, -y+1, z+\frac{1}{2}$; (viii) $x, -y+1, z+\frac{1}{2}$; (ix) $x-\frac{1}{2}, y+\frac{1}{2}, z$.

Bian *et al.*, 2003). Similarly, 3,5-dinitrosalicylic acid (**DN**) is used to detect sugar levels in urine by colorimetric methods (Kumar *et al.*, 2015). The presence of the OH and COOH functional groups in these molecules makes them capable of forming a variety of supramolecular synthons. **DB** readily forms solvates or hydrates and cocrystals with active pharmaceutical ingredients (APIs) (Mazurek *et al.*, 2007). Similarly, NO_2-substituted benzoic acids have been shown to be efficient proton-donor and electron-transfer species in adduct formation (Smith *et al.*, 1995). The formation of salt and cocrystal forms of an API depends on the ΔpK_a value (Kumar & Nanda, 2017). Proton transfer will occur when the pK_a value is greater than 2 or 3. In our case, the ΔpK_a value of **I** is 2.03 and that of **II** is 4.05.

In many crystal structures of salts and cocrystal forms of APIs, water molecules play an important role in the supramolecular packing due to their ability to form hydrogen bonds, both as donors and as acceptors (Krishnaswamy *et al.*, 2014; Babu & Nangia, 2006; Varughese & Desiraju, 2010). In the present study, the crystallized water molecules play an important role in the crystal packing of **I**.

2. Experimental

2.1. Synthesis and crystallization

5-Aminotetrazole and all the other reagents and solvents were used without further purification. Cocrystal **I** and salt **II** were prepared by mixing a hot aqueous solution of 5-aminotetrazole (0.0212 g) with a hot aqueous solution of either 3,5-dihydroxybenzoic acid (**DB**; 0.0385 g) or 3,5-dinitrosalicylic acid (**DN**; 0.0570 g) in a 1:1 equimolar ratio. The mixtures were warmed over a water bath for half an hour at 90 °C. Each of the mixtures was then allowed to cool slowly to room temperature. After a few days, colourless prismatic crystals of **I** and yellow plate-like crystals of **II** could be separated from the mother solution.

2.2. Refinement

Crystal data, data collection and structure refinement details for **I** and **II** are summarized in Table 1. H atoms on C atoms were positioned geometrically (C—H = 0.93) and refined as riding, with U_{iso}(H) = 1.2U_{eq}(C). The amine, hydroxy and water H atoms were placed in the positions indicated by a difference electron-density map, and their positions were allowed to refine together with individual isotropic displacement parameters. All N—H and O—H distances were restrained to 0.98 Å. The water H atoms in **I** were refined with U_{iso}(H) = 1.5U_{eq}(O). The absolute structure parameter in **I**

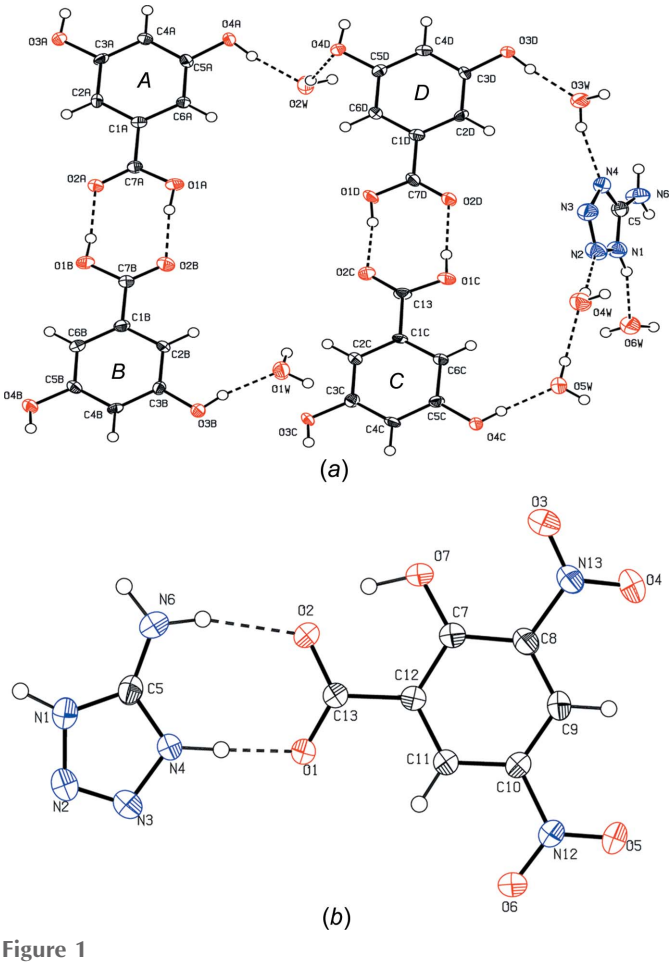

Figure 1
Displacement ellipsoid plots (with the atom-numbering schemes) of the asymmetric units of (*a*) cocrystal **I** and (*b*) salt **II**. Displacement ellipsoids are drawn at the 50% probability level. Dashed lines indicate hydrogen bonds.

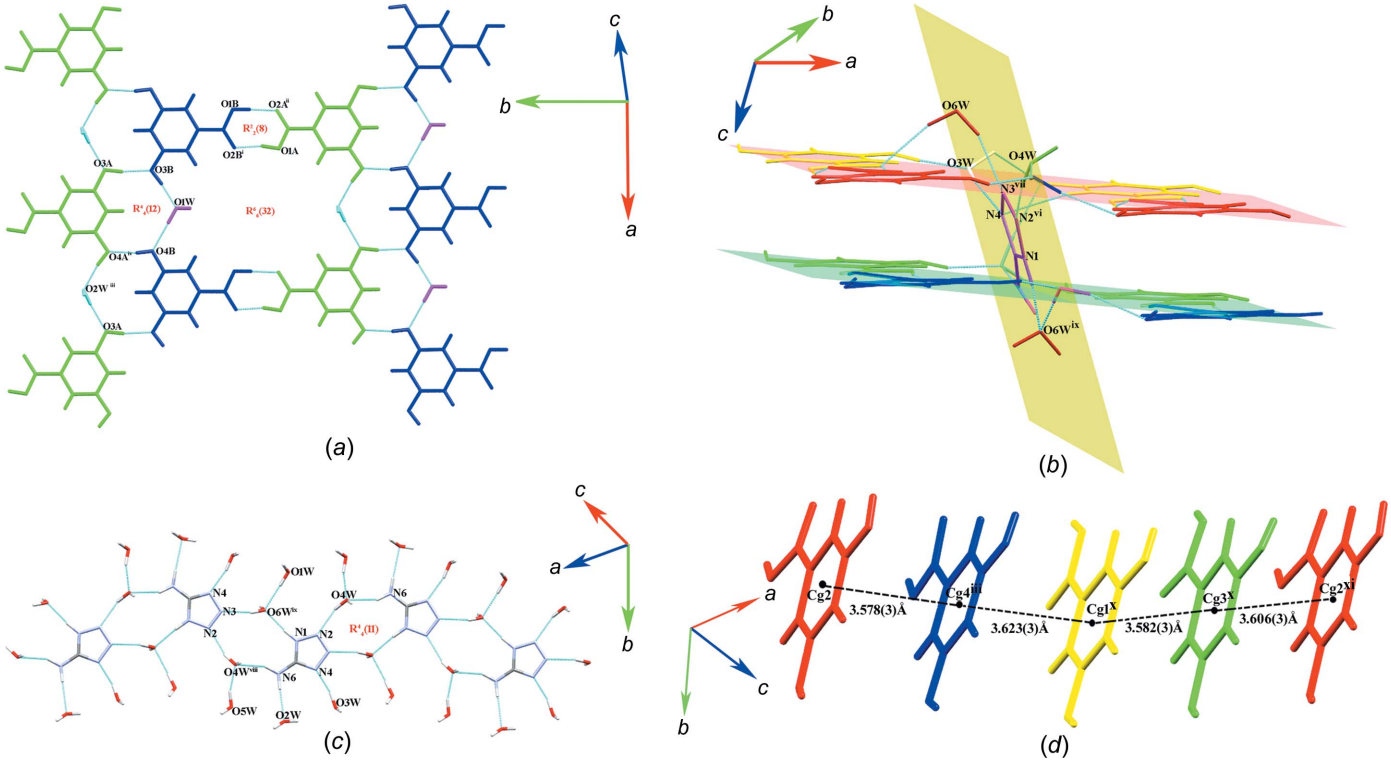

Figure 2
(*a*) The acid layer formed through intermolecular interactions between *A* and *B* molecules along the *a* axis in **I**, with dashed lines representing hydrogen bonds. [Symmetry codes: (i) $x+\frac{1}{2}, y+\frac{1}{2}, z$; (ii) $x-\frac{1}{2}, y-\frac{1}{2}, z$; (iii) $x+1, y, z$; (iv) $x-1, y, z$.] (*b*) Adjacent supramolecular layers connected *via* N—H···O hydrogen bonds. [Symmetry codes: (vi) $x+\frac{1}{2}, y-\frac{1}{2}, z$; (vii) $x+1, -y+1, z+\frac{1}{2}$; (ix) $x-\frac{1}{2}, y+\frac{1}{2}, z$.] (*c*) Hydrogen bonds formed between AT and water in the channels along the *ac* diagonal axis. [Symmetry codes: (viii) $x, -y+1, z+\frac{1}{2}$; (ix) $x-\frac{1}{2}, y+\frac{1}{2}, z$.] (*d*) Adjacent chains interconnected *via* π–π stacking interactions along the *ac* diagonal axis. [Symmetry codes: (iii) $x+1, y, z$; (x) x, y, z; (xi) $x, y, z-1$.]

was meaningless (Table 1). The data for **II** exhibited non-merohedral twinning, with a ratio of the twin components of 0.5208 (14):0.4792 (14).

3. Results and discussion

3.1. 5-Aminotetrazole–3,5-dihydroxybenzoic–water (1/4/6) (I)

Cocrystal **I** crystallizes in the monoclinic space group *Cc* with one **AT**, four **DB** and six water molecules (1:4:6 ratio) in the asymmetric unit, as shown in Fig. 1(*a*). Here, **AT** crystallizes in the amine tautomeric form (see **b** in Scheme 1). In **I**, all the carboxylic acid groups exist in a planar geometry, with the torsion angles ranging from −172.0 (5) to −178.2 (5)°. The acid groups are able to interact through several O—H···O hydrogen bonds, in conjunction with some of the water molecules, to form supramolecular sheets. Acid molecules *A* and *B* form two linked trimeric units *BAB* and *ABA* *via* hydrogen bonds from hydroxy groups (Table 2) to water molecules O1*W* and O2*W*, giving an $R_4^4(12)$ motif. The arrangement of alternating *BAB* and *ABA* groups extends as a strand along the *a* axis. Neighbouring strands link to the first by pairs of O—H···O hydrogen bonds between carboxylic acid groups. This arrangement leads to the formation of a fork-like dimer with an $R_2^2(8)$ graph set. The combination of $R_4^4(12)$ and $R_2^2(8)$

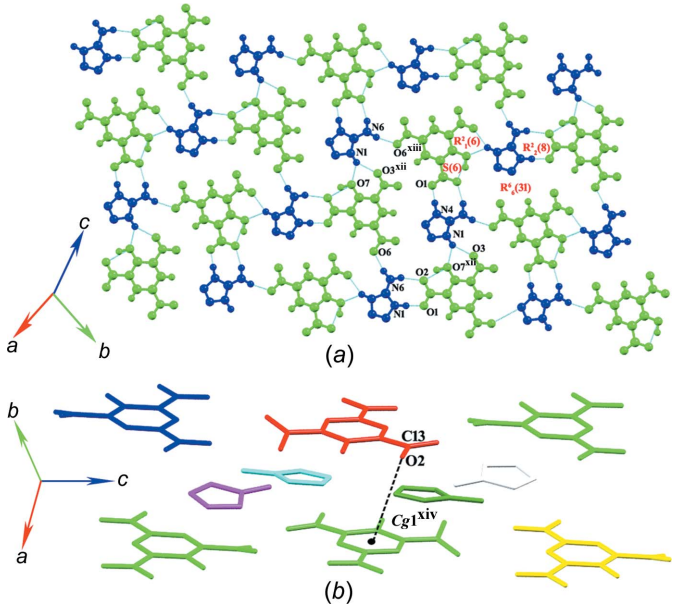

Figure 3
(*a*) The 1D supramolecular sheet formed through N—H···O and O—H···O inter- and intramolecular interactions along the *bc* plane in **II**, with dashed lines representing hydrogen bonds. [Symmetry codes: (xii) $x, -y+\frac{1}{2}, z-\frac{1}{2}$; (xiii) $x, y-1, z$.] (*b*) Adjacent sheets interconnected *via* C═O···π interactions (*Cg*1 is the centroid of the aromatic ring of the anion). [Symmetry code: (xiv) $-x+1, -y+1, -z+1$.]

motifs generates a motif of type $R_6^6(32)$ [Fig. 2(*a*)]. An equivalent set of sheets showing the same graph-set motifs is formed by the interaction of **DB** molecules *C* and *D* with water molecules O3*W* and O5*W* (see Fig. S1 in the supporting information). All of these sheets lie in the *ab* plane.

These two similar sheets are arranged alternately along the *c* axis. Different sheets are connected by N—H···O and O—H···N hydrogen bonds between **AT** molecules and water, as well as by further O—H···O hydrogen bonds from water molecules (Table 2). In this structure, the **AT** molecule does not interact directly with the acid, but interacts through water molecules [Fig. 2(*b*)].

The hydrogen bonds between water molecules O4*W* and O6*W* and two molecules of **AT**, arranged in a head-to-tail fashion, give rise to rings showing an $R_4^4(11)$ motif. These interactions lead to the formation of one-dimensional (1D) supramolecular chains, propagating along the *ac* diagonal axis [Fig. 2(*c*)].

Individual adjacent hydrogen-bonded sheets pack in an offset fashion such that the large $R_6^6(32)$ ring motifs align to form zigzag channels running along the *ac* diagonal axis. These channels are occupied by hydrogen-bonded chains of **AT** and water. A three-dimensional (3D) supramolecular architecture is formed when all of the hydrogen-bonding interactions are considered. The supramolecular architecture is further stabilized by aromatic π–π stacking interactions between the benzene rings of **DB** molecules in adjacent sheets [Fig. 2(*d*)], with centroid–centroid distances ranging between 3.579 (3) and 3.623 (3) Å, and angles between the aromatic ring planes varying between 1.5 (3) and 3.2 (3)°. The interactions form π-stacked chains of **DB** molecules running along the *ac* diagonal axis.

Table 3
Hydrogen-bond geometry (Å, °) for **II**.

D—H···*A*	*D*—H	H···*A*	*D*···*A*	*D*—H···*A*
O7—H7···O2	1.00 (1)	1.52 (1)	2.4576 (15)	155 (2)
N1—H1···O3^{xii}	0.96 (1)	2.10 (2)	2.967 (2)	150 (2)
N1—H1···O7^{xii}	0.96 (1)	2.09 (2)	2.8033 (17)	130 (2)
N4—H4···O1	0.99 (1)	1.58 (1)	2.5668 (17)	178 (2)
N6—H6*A*···O6^{xiii}	0.94 (1)	1.94 (1)	2.8643 (19)	167 (2)
N6—H6*B*···O2	0.95 (1)	2.02 (1)	2.9367 (19)	164 (2)

Symmetry codes: (xii) $x, -y+\frac{1}{2}, z-\frac{1}{2}$; (xiii) $x, y-1, z$.

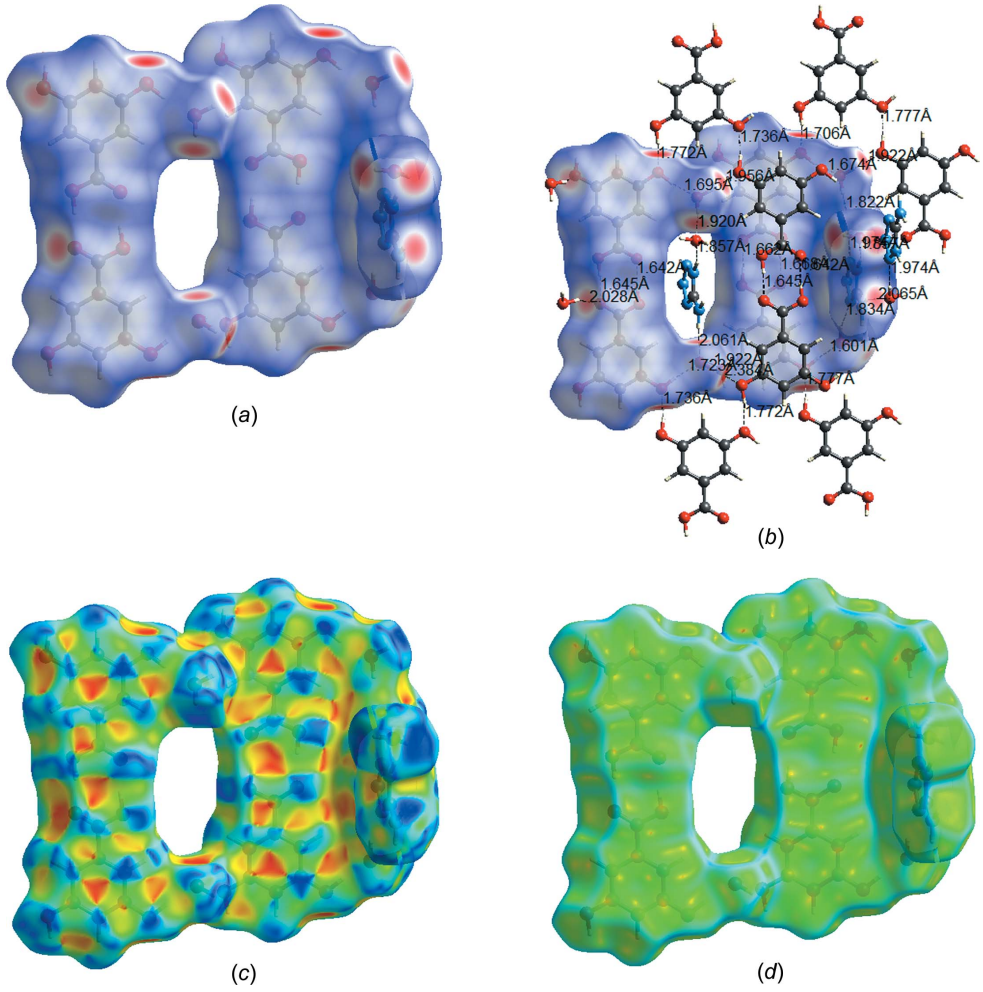

Figure 4
(*a*) Hirshfeld surface generated over d_{norm} for cocrystal **I**. (*b*) Intermolecular interactions with the 2D Hirshfeld surface generated for cocrystal **I**. (*c*) Shape index and (*d*) curvedness mapped over the Hirshfeld analysis.

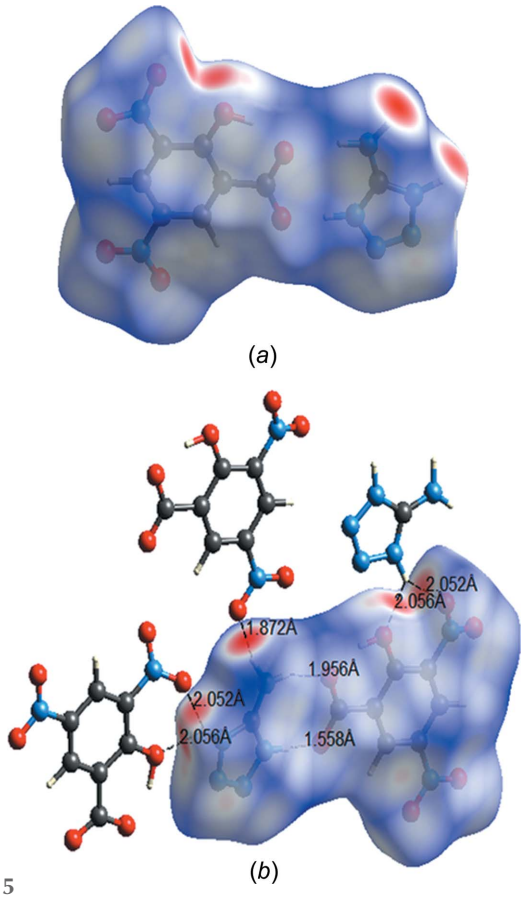

Figure 5
(*a*) Hirshfeld surface generated over d_{norm} for salt **II**. (*b*) Intermolecular interactions with the 2D Hirshfeld surface generated for salt **II**.

3.2. 5-Aminotetrazolium 3,5-dinitrosalicylate (II)

Salt **II** crystallizes in the monoclinic space group $P2_1/c$ with one **AT** cation and one **DN** anion in the asymmetric unit [Fig. 1(*b*)]. Here, **AT** crystallizes in the amine tautomeric form (see **b** in Scheme 1) and is protonated at the N4 position. The **AT** cation and **DN** anion are nearly coplanar [the angle between the planes of the C_6 and CN_4 rings is 7.80 (8)°]. The deprotonated carboxylate group is coplanar with the benzene ring, with a torsion angle of 178.63 (15)°, as is one of the nitro groups [torsion angle of 179.14 (15)°]. The other nitro group adopts a less coplanar arrangement, with a torsion angle of 17.9 (2)°. The **AT** cation interacts with the **DN** anion through N—H···O hydrogen bonds in several ways, resulting in the formation of supramolecular sheets. First, there is a hydrogen-bonding interaction between a protonated ring N atom, the amine group and the carboxylate group (Table 3), which forms a dimer with graph set $R_2^2(8)$. Second, the other protonated ring N atom acts as a bifurcated hydrogen-bond donor and forms a pair of hydrogen bonds to the other nitro group and the hydroxy group, resulting in an $R_1^2(6)$ ring motif. A typical intramolecular O—H···O hydrogen bond also exists between the hydroxy group and a carboxylate O atom of the **DN** anion, with an $S(6)$ motif [Fig. 3(*a*)]. The combination of $R_2^2(8)$, $R_1^2(6)$ and $S(6)$ motifs leads to the formation of a hexameric unit (involving three **AT** and three **DN** molecules), with a graph-set motif of $R_6^6(31)$, within the two-dimensional (2D) sheets and extending along the *bc* plane.

The offset between adjacent sheets in this structure does not allow for the formation of π–π interactions; however, the supramolecular sheets are weakly connected by C=O(carbonyl)···π interactions, with an O···centroid distance of 3.7012 (13) Å [Fig. 3(*b*)].

3.3. Hirshfeld surface analysis

The Hirshfeld surface (HS) and 2D fingerprint plots (Hirshfeld, 1977; Spackman & McKinnon, 2002; Spackman & Jayatilaka, 2009) were generated (Wolff *et al.*, 2012; Venkatesan *et al.*, 2016) for **I** and **II**. In cocrystal **I** and salt **II**, the HS indicates that the key intermolecular interactions in the molecules are a selection of N—H···O, O—H···O and O—H···N interactions present in each structure [Figs. 4(*a*), 4(*b*), 5(*a*) and 5(*b*)]. The HS map of shape index [Fig. 4(*c*)] visualizes the π–π stacking present in the structure of cocrystal **I** (Seth *et al.*, 2011). The curvedness in the crystal structure shows the stacking of molecules in 3D space by the presence of a flat green region [Fig. 4(*d*)] (Soman *et al.*, 2014).

The 2D fingerprint plots calculate and visualize the proportion of different types of intermolecular interactions in

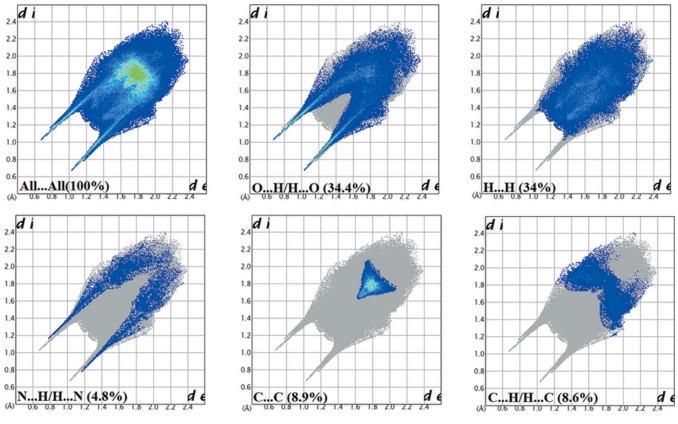

Figure 6
Hirshfeld surface analysis and 2D fingerprint plots for cocrystal **I**.

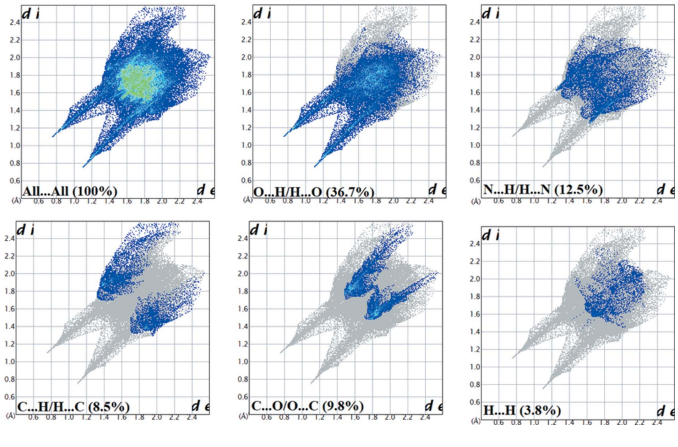

Figure 7
Hirshfeld surface analysis and 2D fingerprint plots for cocrystal **II**.

Table 4
Crystallographic and interaction details of compounds **I** and **II** and some known related structures.

Ligand	Acid	Space group; unit-cell parameters (Å, °)	Primary interaction	Graph-set motif	Motif type	Secondary interaction	Graph-set motif	Motif type
5-Aminotertrazole	Hydrochloride	*Pbca*; *a* = 7.63530 (10), *b* = 11.3272 (2), *c* = 12.8959	N—H···Cl	$R_2^1(6)$	I	N—H···Cl, N—H···O	$R_4^2(10)$ and $R_4^3(10)$	VII and VIII
	Hydrobromide	*Pbcm*; *a* = 6.5473 (2), *b* = 7.7505 (2), *c* = 11.5478 (4)	N—H···Br	$R_2^1(6)$	I	N—H···Br, O—H···Br	$R_6^4(15)$	VI
	Iodide	*Pbcm*; *a* = 6.84660 (10), *b* = 7.8770 (2), *c* = 12.0820 (2)				N—H···I, O—H···I	$R_6^4(15)$	VI
	Nitrate	$P2_1/c$; *a* = 10.5493 (8), *b* = 3.4556 (4), *c* = 14.606 (1), *β* = 90.548 (9)	N—H···O	$R_2^2(6)$	II	N—H···O	$R_2^1(4)$ and $R_2^2(4)$	IX
	Perchlorate	$P2_1/n$; *a* = 5.26150 (10), *b* = 8.5311 (2), *c* = 21.4870 (4), *β* = 96.1273 (13)	N—H···N	$R_2^2(6)$	III	N—H···O	$R_2^2(8)$	XII
	Picrate	*C*2/*c*; *a* = 25.4959 (13), *b* = 6.1793 (3), *c* = 14.5863 (8), *β* = 98.069 (1)	N—H···O	$R_2^1(6)$	I	N—H···O	$R_1^2(6)$ and $R_1^2(4)$	X and XI
	3,5-Dihydroxy-benzoic acid, **I**	*Cc*; *a* = 9.4539 (6), *b* = 29.9892 (15), *c* = 13.1934 (10), *β* = 106.454 (7)	N—H···O, O—H···O	$R_4^4(11)$	V			
	3,5-Dinitro-salycylic acid, **II**	$P2_1/c$; *a* = 6.2591 (3), *b* = 11.1312 (5), *c* = 17.2257 (9), *β* = 98.646 (5)	N—H···O	$R_2^2(8)$	IV	N—H···O	$R_1^2(6)$ and $R_6^6(31)$	X and XIII

the crystal structures of **I** and **II** (Figs. 6 and 7). The breakdown of the contributions to the interactions in cocrystal **I** and salt **II** are O···H/H···O (**I** 34.4%, **II** 36.7%), N···H/H···N (**I** 4.8%, **II** 12.5%), C···H/H···C (**I** 8.6%, **II** 8.5%), H···H (**I** 34.0%, **II** 3.8%), C···C (**I** 8.9%) and C···O (**II** 9.8%). The fingerprint plots show that O—H···O hydrogen bonds are the major contributor to the interactions in both structures, with O···H/H···O 34.4% in **I** and 36.7% in **II**.

3.3.1. Comparative analysis. Data for the crystal structures and hydrogen-bonding motifs in **I** and **II**, as well as for the known related compounds **AT** nitrate, **AT** halogenides (von Denffer *et al.*, 2008), **AT** perchlorate (Klapötke *et al.*, 2008) and **AT** picrate (Jin *et al.*, 2005), are presented in Table 4. The hydrogen-bonding motifs observed in these compounds are presented in Figs. 8 and 9. In most of the crystal structures involving **AT**, the tetrazole ring exists with a planar geometry.

In **I**, the primary interactions involving **AT** are all to water *via* N—H···O and O—H···N hydrogen bonds, and result in the formation of an $R_4^4(11)$ (type V) motif. In contrast, in the structure of salt **II**, the **AT** cation forms primary interactions with the **DN** anion *via* N—H···O hydrogen bonds, and gives rise to an $R_2^2(8)$ (type IV) motif. A secondary $R_1^2(6)$ (type X) motif is also found, which combines with the other interactions to give an $R_6^6(31)$ (type XIII) motif. The supramolecular motifs in **II** are similar to those observed in the structure of **AT** picrate (Jin *et al.*, 2005).

In **AT** salts, motifs of types III, VI and IX are predominant. A comparison of the halide salts shows that the bromide and iodide are isomorphous, but that the chloride adopts a different structure. Despite this, both the chloride and the bromide show primary interactions of type I, while the iodide does not show any primary interaction motif. However, when the secondary pattern of interactions is considered, the chloride shows interactions of types VII and VIII, whereas in the bromide and iodide, the interactions are of type VI. In the nitrate salt, the cation and anion interact directly with each other and form $R_2^2(6)$ (type II), $R_2^2(4)$ (type IX) and $R_2^1(4)$ (type XI) motifs.

In the perchlorate salt, **AT** forms two motifs, *i.e.* $R_2^2(6)$ (type III) and $R_2^2(8)$ (type XII). One of these forms between two **AT** bases and the other forms between an **AT** cation and a perchlorate anion. When it comes to the case of the picrate salt, the acid anion interacts with the **AT** cation and forms $R_2^1(6)$ (type I), $R_1^2(6)$ (type X) and $R_1^2(4)$ (type XI) motifs.

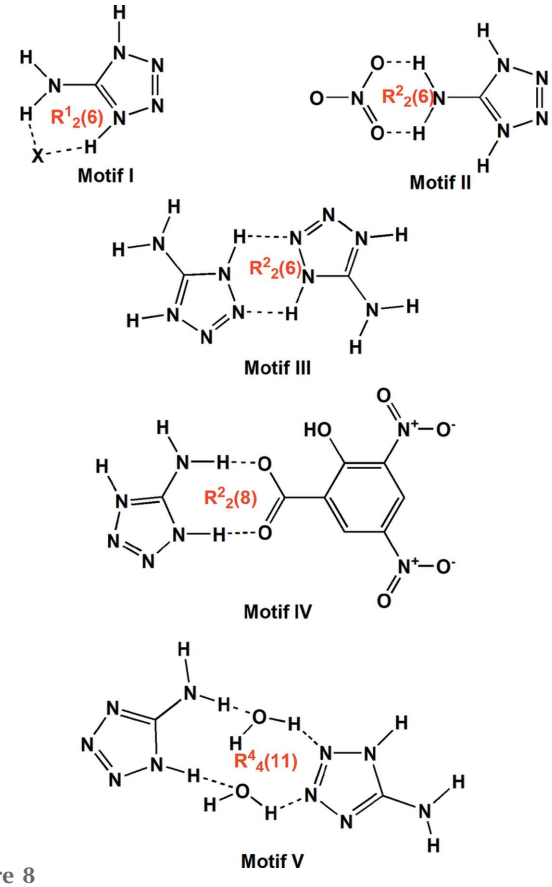

Figure 8
Hydrogen-bonding motifs I–V observed in known related compounds of **I** and **II**.

A comparative study of the salt forms of **AT** reveals a wide range of different types of graph-set motifs arising through different molecular recognition patterns. The most commonly observed primary motif is $R_2^2(8)$.

AT forms different types of hydrogen bonds, including N—H···Br, N—H···Cl, N—H···I, N—H···N and N—H···O, with the acid anions. A comparison of the hydrogen-bond geometry of **AT** in **I** and **II**, and in the previously reported salt forms (von Denffer *et al.*, 2008; Klapötke *et al.*, 2008; Jin *et al.*, 2005), is given in Table 5. The comparison shows that the N—

Table 5
A comparison of the hydrogen-bond geometry (Å, °) of **AT** in different solid forms.

Compound	D—H···A	$d(D\cdots A)$	$\angle(D$—H···$A)$
Aminotetrazolium bromide	N—H···Br	3.4091 (5)	154 (2)
Aminotetrazolium iodide	N—H···I	3.588 (2)	161 (4)
Aminotetrazolium chloride	N—H···Cl	3.242 (2)	170 (2)
Aminotetrazole with solvents	N—H···O	2.772 (2)	152 (2)
	N—H···O	2.755 (2)	146 (2)
	N—H···O	2.667 (2)	165 (2)
N—H···N interaction in aminotetrazole	N—H···N	2.819 (2)	159 (2)
	N—H···N	2.861 (2)	150 (2)
	N—H···N	3.073 (2)	125 (2)
	N—H···N	3.074 (2)	111 (1)
	N—H···N	3.026 (2)	125 (2)
	N—H···N	3.039 (2)	114 (2)
	N—H···N	3.068 (3)	113 (2)
	N—H···N	3.185 (3)	116 (2)
Aminotetrazolium nitrate	N—H···O	2.7527 (14)	172.7 (18)
	N—H···O	2.7653 (14)	177.2 (18)
Aminotetrazolium perchlorate	N—H···O	2.931 (3)	167 (3)
	N—H···O	2.973 (2)	168 (2)
Aminotetrazolium picrate	N—H···O	3.0105 (13)	152
	N—H···O	2.9999 (13)	169
Aminotetrazole in cocrystal **I**	N—H···O	2.837 (6)	172 (5)
	N—H···O	3.065 (5)	177 (6)
Aminotetrazole in salt **II**	N—H···O	2.8643 (19)	163.7 (17)
	N—H···O	2.8643 (19)	167.4 (19)
	N—H···O	2.5668 (17)	178 (2)

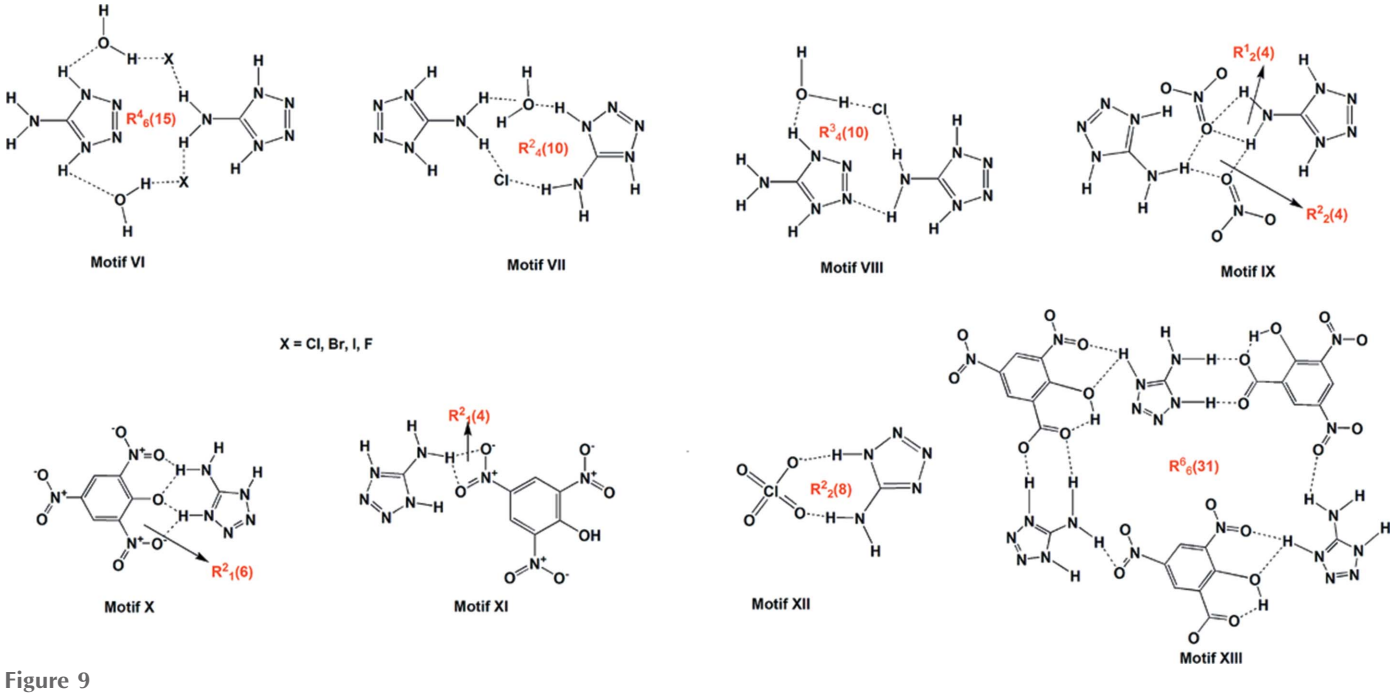

Figure 9
Hydrogen-bonding motifs VI–XIII observed in known related compounds of **I** and **II**.

Table 6
pK_a values of acids and base, and ΔpK_a between acids and base.

Acids/base	pK_a	Product from the reaction of **AT** with acid	ΔpK_a	Compound type
5-Aminotetrazole (**AT**)	6.0			
HBr	−9	5-Aminotrerazolium hydrobromide	15	Salt
HCl	−7	Aminotetrazolium chloride	13	Salt
HI	−9.3	Aminotetrazolium iodide	15.3	Salt
NO_3	−1.3	Aminotetrazolium nitrate	7.3	Salt
ClO_4	−10	Aminotetrazolium perchlorate	16	Salt
Picric acid	0.38	Aminotetrazolium picrate	5.68	Form I Salt; Form II Cocrystal
3,5-Dihydroxybenzoic acid	4.04	5-Aminotetrazole–3,5-dihydroxybenzoic acid	1.96	Cocrystal
3,5-Dinitrosalicylic acid	2.02	5-Aminotetrazole–3,5-dinitrosalicylic acid	3.98	Salt

H···O hydrogen bonds predominte. The donor–acceptor distances, $d(D\cdots A)$, of the N—H···A hydrogen bonds vary between 2.667 (2) and 3.0105 (13) Å, and the D—H···A angle varies between 146 (2) and 178 (2)°. The $d(D\cdots A)$ of the N—H···N base pairing varies from 2.819 (2) to 3.185 (3) Å, and the D—H···O angle varies from 111 (1) to 159 (2)°. Similarly, for the N—H···Br, N—H···Cl and N—H···I hydrogen bonds, the $d(D\cdots A)$ distance varies from 3.242 (2) to 3.588 (2) Å and the D—H···A angle varies from 154 (2) to 170 (2)°.

It can be seen that the majority of the known solid forms of **AT** are salts. Since the ΔpK_a value determines the formation of a salt or cocrystal, when the ΔpK_a value is greater than 2 or 3, salt formation is expected, and when the ΔpK_a value is less than 2, cocrystal formation is expected (Cruz-Cabeza, 2012). Based on this information, the ΔK_a values in the **AT** solid forms were calculated and are listed in Table 6. Our comparison confirmed that salt and cocrystal formation in **AT** solid forms abide by the rule. The only deviation is in the case of picric acid. Though the ΔpK_a value suggests that salt formation is the only possibility, a cocrystal form is also known to exist. This has been attributed to the choice of solvent used for crystallization (Rager & Hilfiker, 2010).

4. Conclusion

New cocrystal and salt forms of **AT** have been synthesized with 3,5-dihydroxybenzoic acid and 3,5-dinitrosalicylic acid, respectively, and the formation of the cocrystal and salt forms of **AT** have been confirmed by the pK_a value. Amine form **b** (see Scheme 1) crystallizes in both crystal structures. In cocrystal **I**, the **AT** molecule does not interact directly with the **DB** molecule; instead, interactions are mediated through water molecules. The presence of water molecules in the lattice has disrupted the direct interaction of **AT** with **DB**. The **DB** molecules interact with each other and with water molecules *via* hydrogen bonds, giving $R_2^2(8)$, $R_4^4(12)$ and $R_6^6(32)$ motifs. In contrast, in salt **II**, with no cocrystallized water, the **AT** cation interacts directly with the **DN** anion through N—H···O hydrogen bonds and forms dimers with an $R_2^2(8)$ motif. In both crystal structures, **AT** exists with a planar geometry, which leads to **AT** and water forming a 1D supramolecular chain in **I** and a 3D sheet-like arrangement in **II**. Both compounds show further hydrogen-bonding interactions, giving rise to a 3D supramolecular architecture (in **I**) or 2D sheets (in **II**). A Hirshfeld surface analysis shows that O—H···O and N—H···O hydrogen bonds are the major contributors to the formation of supramolecular architectures in these structures (**I** 34.4% and **II** 36.7%).

References

Adams, V. H., Bazar, M. A., Reinke, E. N., Buckalew, A. R. & Eck, W. S. (2020). *Regul. Toxicol. Pharmacol.* **111**, 1–7.
Albert, A., Goldacre, R. & Phillips, J. (1948). *J. Chem. Soc.* pp. 2240–2249.
Allen, F. H., Johnson, O., Shields, G. P., Smith, B. R. & Towler, M. (2004). *J. Appl. Cryst.* **37**, 335–338.
Aromi, G., Barrios, L. A., Roubeau, O. & Coord, G. P. (2011). *Chem. Rev.* **255**, 485–546.
Babu, N. J. & Nangia, A. (2006). *Cryst. Growth Des.* **6**, 1753–1756.
Bian, S., Doh, H. J., Zheng, J., Kim, J. S., Lee, C. H. & Kim, D. D. (2003). *Eur. J. Pharm. Sci.* **18**, 141–147.
Boraei, A. A. A. (2001). *J. Chem. Eng. Data*, **46**, 939–943.
Bradbury, R. H., Allott, C. P., Dennis, M., Girdwood, J. A., Kenny, P. W., Major, J. S., Oldham, A. A., Ratcliffe, A. H., Rivett, J. E., Roberts, D. A., *et al.* (1993). *J. Med. Chem.* **36**, 1245–1254.
Bray, D. D. & White, J. G. (1979). *Acta Cryst.* B**35**, 3089–3091.
Britts, K. & Karle, I. L. (1967). *Acta Cryst.* **22**, 308–312.
Budevich, V. A., Voitekhovich, S. V., Zuraev, A. V., Matulis, V. E., Matulis, V. E., Lyakhov, A. S., Ivashkevich, L. S. & Ivashkevich, O. A. (2021). *Beilstein J. Org. Chem.* **17**, 385–395.
Butler, R. N. (1977). *Adv. Heterocycl. Chem.* **21**, 323–435.
Cason, C. J. (2004). *POV-RAY for Windows*. Persistence of Vision, Raytracer Ptv. Ltd, Victoria, Australia. http://www.povray.org/.
Cruz-Cabeza, A. J. (2012). *CrystEngComm*, **14**, 6362–6365.
Denffer, M. von, Klapötke, T. M. & Miró Sabaté, C. (2008). *Z. Anorg. Allg. Chem.* **634**, 2575–2582.
Ernst, V., Klapötke, T. M. & Stierstorfer, J. (2007). *Z. Anorg. Allg. Chem.* **633**, 879–887.
Fujihisa, H., Honda, K., Obata, S., Yamawaki, H., Takeya, S., Gotoh, Y. & Matsunaga, T. (2011). *CrystEngComm*, **13**, 99–102.
Hirshfeld, F. L. (1977). *Theor. Chim. Acta*, **44**, 129–138.
Jin, C. H., Ye, C., Piekarski, C., Twamley, B. & Shreeve, J. M. (2005). *Eur. J. Inorg. Chem.* **2005**, 3760–3767.
Katritzky, A. R. & Lagowski, J. M. (1963). *Adv. Heterocycl. Chem.* **2**, 27–81.
Kawase, M., Motohashi, N., Kurihara, T., Inagaki, M., Satoh, K. & Sakagami, H. (1988). *Anticancer Res.* **18**, 1069–1074.
Kiselev, V. G. & Gritsan, N. P. (2009). *J. Phys. Chem. A*, **113**, 3677–3684.
Klapötke, T. M., Sabaté, C. M. & Stierstorfer, J. (2008). *Z. Anorg. Allg. Chem.* **634**, 1867–1874.
Krishnaswamy, G., Suchetan, P. A., Sreenivasa, S., Naveen, S., Lokanath, N. K. & Aruna Kumar, D. B. (2014). *Acta Cryst.* E**70**, 541–543.
Kumar, A., Pandith, A. & Kim, H. S. (2015). *Dyes Pigments*, **122**, 351–358.
Kumar, S. & Nanda, A. (2017). *Indian J. Pharm. Sci.* **79**, 858–871.

Levchik, S. V., Ivashkevich, O. A., Balabanovich, A. I., Lesnikovich, A. I., Gaponik, P. N. & Costa, L. (1992). *Thermochim. Acta*, **207**, 115–130.
Li, Q.-Y., Yang, G.-W., Yuan, R.-X., Wang, J.-P. & Cui, P.-F. (2008). *Acta Cryst.* C**64**, m26–m29.
Li, Y., Zhang, X., Lan, J., Xu, P. & Sun, J. (2019). *Inorg. Chem.* **58**, 13917–13926.
Macrae, C. F., Sovago, I., Cottrell, S. J., Galek, P. T. A., McCabe, P., Pidcock, E., Platings, M., Shields, G. P., Stevens, J. S., Towler, M. & Wood, P. A. (2020). *J. Appl. Cryst.* **53**, 226–235.
Mazurek, J., Dova, E. & Helmond, R. (2007). *Acta Cryst.* E**63**, o3289.
Mishra, R. & Pallepogu, R. (2018). *Acta Cryst.* B**74**, 32–41.
Neochoritis, C. G., Zhao, T. & Dömling, A. (2019). *Chem. Rev.* **119**, 1970–2042.
Parsons, S., Flack, H. D. & Wagner, T. (2013). *Acta Cryst.* B**69**, 249–259.
Rager, T. & Hilfiker, R. (2010). *Cryst. Growth Des.* **10**, 3237–3241.
Rigaku (2015). *CrystalClear*. Rigaku Americas, The Woodlands, Texas, USA, and Rigaku Corporation, Tokyo, Japan.
Rigaku OD (2019). *CrysAlis PRO*. Rigaku Oxford Diffraction Ltd, Yarnton, Oxfordshire, England.
Seth, S. K., Maity, G. C. & Kar, T. (2011). *J. Mol. Struct.* **1000**, 120–126.
Sheldrick, G. M. (2015*a*). *Acta Cryst.* A**71**, 3–8.
Sheldrick, G. M. (2015*b*). *Acta Cryst.* C**71**, 3–8.
Sinditskii, V. P., Fogelzang, A. E., Levshenkov, A. I., Egorshev, V. Y., Kolesov, V. I. & Serushkin, V. V. (1995). *Proceedings of the 21st International Pyrotechnics Seminar*, pp. 762–773.
Singh, H., Chawla, A. S., Kapoor, U. K., Paul, D. & Malhotra, R. K. (1980). *Prog. Med. Chem.* **17**, 151–183.
Smith, G., Lynch, D. E., Byriel, K. A. & Kennard, C. H. L. (1995). *Aust. J. Chem.* **48**, 1133–1149.
Soman, R., Sujatha, S. & Arunkumar, C. (2014). *J. Fluor. Chem.* **163**, 16–22.
Spackman, M. A. & Jayatilaka, D. (2009). *CrystEngComm*, **11**, 19–32.
Spackman, M. A. & McKinnon, J. J. (2002). *CrystEngComm*, **4**, 378–392.
Spek, A. L. (2020). *Acta Cryst.* E**76**, 1–11.
Torii, H., Nakadai, M., Ishihara, K., Saito, S. & Yamamoto, H. (2004). *Angew. Chem. Int. Ed.* **43**, 1983–1986.
Upadhayaya, R. S., Jain, S., Sinha, N., Kishore, N., Chandra, R. & Arora, S. K. (2004). *Eur. J. Med. Chem.* **39**, 579–592.
Varughese, S. & Desiraju, G. R. (2010). *Cryst. Growth Des.* **10**, 4184–4196.
Venkatesan, P., Thamotharan, S., Ilangovan, A., Liang, H. & Sundius, T. (2016). *Spectrochim. Acta A Mol. Biomol. Spectrosc.* **153**, 625–636.
Wolff, S. K., Grimwood, D. J., McKinnon, J. J., Turner, M. J., Jayatilaka, D. & Spackman, M. A. (2012). *CrystalExplorer17*. University of Western Australia. https://crystalexplorer.scb.uwa.edu.au/.
Yang, Q., Chen, S., Xie, G. & Gao, S. (2012). *J. Coord. Chem.* **65**, 2584–2592.
Zhang, J. G., Feng, L. N., Shu, Y. J., Zhang, S. W., Zhang, T. L., Yang, L. & Wu, M. (2009). *J. Mol. Model.* **15**, 67–77.

supporting information

Acta Cryst. (2022). C**78**, 414-423 [https://doi.org/10.1107/S2053229622006519]

Structure determination and Hirshfeld surface analysis of new cocrystal and salt forms of 5-aminotetrazole with hydroxy- and nitro-substituted carboxylic acids

Jeyaraman Selvaraj Nirmal Ram, Udhayasuriyan Sathya, Sundaramoorthy Gomathi and David Bradford Cordes

Computing details

For both structures, data collection: *CrystalClear-SM Expert* (Rigaku, 2015); cell refinement: *CrysAlis PRO* (Rigaku OD, 2019); data reduction: *CrysAlis PRO* (Rigaku OD, 2019); program(s) used to solve structure: SHELXT2018 (Sheldrick, 2015a); program(s) used to refine structure: *SHELXL2018* (Sheldrick, 2015b); molecular graphics: *Mercury* (Macrae *et al.*, 2020), *PLATON* (Spek, 2020) and POVRay (Cason, 2004); software used to prepare material for publication: *enCIFer* (Allen *et al.*, 2004).

5-Aminotetrazole–3,5-dihydroxybenzoic acid–water (1/4/6) (I)

Crystal data

$CH_3N_5{\cdot}4C_7H_6O_4{\cdot}6H_2O$
M_r = 809.65
Monoclinic, *Cc*
a = 9.4539 (6) Å
b = 29.9892 (15) Å
c = 13.1934 (10) Å
β = 106.454 (7)°
V = 3587.3 (4) Å^3
Z = 4
F(000) = 1696
D_x = 1.499 Mg m^{-3}
Mo *Kα* radiation, *λ* = 0.71073 Å
Cell parameters from 5950 reflections
θ = 2.1–31.9°
μ = 0.13 mm^{-1}
T = 173 K
Prism, colourless
0.21 × 0.14 × 0.04 mm

Data collection

Rigaku SCXMini diffractometer
Radiation source: Sealed Tube
SHINE graphite Monochromator monochromator
ω scans
Absorption correction: multi-scan (CrysAlis PRO; Rigaku OD, 2019)
T_{min} = 0.993, T_{max} = 1.000
22166 measured reflections
11003 independent reflections
5256 reflections with $I > 2\sigma(I)$
R_{int} = 0.060
θ_{max} = 31.8°, θ_{min} = 2.1°
h = −13→13
k = −41→43
l = −19→18

Refinement

Refinement on F^2
Least-squares matrix: full
$R[F^2 > 2\sigma(F^2)]$ = 0.066
$wR(F^2)$ = 0.152
S = 0.98
11003 reflections
601 parameters
30 restraints
Primary atom site location: dual
Hydrogen site location: mixed
H atoms treated by a mixture of independent and constrained refinement

$w = 1/[\sigma^2(F_o^2) + (0.0595P)^2]$
where $P = (F_o^2 + 2F_c^2)/3$
$(\Delta/\sigma)_{max} = 0.001$
$\Delta\rho_{max} = 0.37$ e Å^{-3}
$\Delta\rho_{min} = -0.28$ e Å^{-3}

Absolute structure: Flack *x* determined using 1769 quotients [(I+)-(I-)]/[(I+)+(I-)] (Parsons *et al.*, 2013)
Absolute structure parameter: 0.4 (7)

Special details

Geometry. All e.s.d.'s (except the e.s.d. in the dihedral angle between two l.s. planes) are estimated using the full covariance matrix. The cell e.s.d.'s are taken into account individually in the estimation of e.s.d.'s in distances, angles and torsion angles; correlations between e.s.d.'s in cell parameters are only used when they are defined by crystal symmetry. An approximate (isotropic) treatment of cell e.s.d.'s is used for estimating e.s.d.'s involving l.s. planes.

Fractional atomic coordinates and isotropic or equivalent isotropic displacement parameters (Å²)

	x	*y*	*z*	U_{iso}*/U_{eq}
O1A	0.9818 (4)	0.67388 (12)	0.6014 (3)	0.0318 (9)
H1A	0.967 (7)	0.7064 (9)	0.606 (5)	0.045 (17)*
O1B	0.2417 (4)	0.26327 (12)	0.6126 (4)	0.0371 (10)
H1B	0.246 (8)	0.2309 (9)	0.620 (6)	0.08 (2)*
O1C	0.2331 (4)	0.29583 (13)	0.3553 (3)	0.0318 (10)
H1C	0.220 (7)	0.2640 (10)	0.366 (5)	0.046 (18)*
O1D	0.4968 (4)	0.70591 (13)	0.3795 (3)	0.0317 (10)
H1D	0.500 (6)	0.7379 (9)	0.386 (4)	0.033 (16)*
O1W	0.8376 (4)	0.37670 (11)	0.5850 (3)	0.0349 (10)
H1WA	0.854 (7)	0.3490 (12)	0.623 (4)	0.052*
H1WB	0.927 (4)	0.3923 (18)	0.590 (5)	0.052*
O2A	0.7568 (4)	0.67594 (12)	0.6255 (3)	0.0275 (9)
O2B	0.4791 (4)	0.26096 (12)	0.6142 (3)	0.0340 (10)
O2C	−0.0008 (4)	0.29331 (14)	0.3633 (3)	0.0325 (10)
O2D	0.7196 (4)	0.70819 (13)	0.3529 (3)	0.0295 (9)
O2W	0.3356 (4)	0.56008 (11)	0.5769 (3)	0.0303 (9)
H2WA	0.430 (4)	0.5468 (18)	0.605 (4)	0.045*
H2WB	0.333 (6)	0.5626 (18)	0.503 (2)	0.045*
O3A	0.6138 (4)	0.51485 (12)	0.6269 (3)	0.0286 (9)
H3A	0.619 (8)	0.4828 (11)	0.612 (6)	0.10 (3)*
O3B	0.6019 (4)	0.42532 (12)	0.5830 (3)	0.0253 (8)
H3B	0.681 (5)	0.4062 (18)	0.576 (5)	0.06 (2)*
O3C	−0.1312 (4)	0.45476 (12)	0.3875 (3)	0.0233 (8)
H3C	−0.132 (6)	0.4857 (9)	0.372 (4)	0.041 (17)*
O3D	0.8514 (4)	0.54398 (12)	0.3372 (3)	0.0228 (8)
H3D	0.929 (5)	0.5651 (16)	0.344 (5)	0.054 (18)*
O3W	0.0805 (4)	0.59265 (14)	0.3484 (4)	0.0481 (12)
H3WA	0.098 (8)	0.6226 (12)	0.376 (5)	0.072*
H3WB	0.141 (6)	0.587 (2)	0.303 (4)	0.072*
O4A	1.1046 (4)	0.51122 (12)	0.5934 (3)	0.0273 (9)
H4A	1.185 (5)	0.5309 (17)	0.598 (5)	0.06 (2)*
O4B	0.1211 (4)	0.42277 (12)	0.6339 (3)	0.0257 (8)
H4B	0.121 (7)	0.4536 (11)	0.609 (5)	0.08 (3)*
O4C	0.3506 (4)	0.45786 (13)	0.3371 (3)	0.0290 (9)

H4C	0.429 (5)	0.4368 (15)	0.348 (4)	0.042 (16)*
O4D	0.3609 (4)	0.54587 (12)	0.3697 (3)	0.0283 (9)
H4D	0.370 (5)	0.5154 (9)	0.360 (4)	0.018 (13)*
O4W	0.6163 (4)	0.32244 (12)	0.2974 (3)	0.0383 (9)
H4WA	0.630 (7)	0.3028 (17)	0.357 (3)	0.058*
H4WB	0.678 (6)	0.3175 (19)	0.254 (4)	0.058*
O5W	0.5802 (4)	0.41320 (13)	0.3215 (3)	0.0375 (10)
H5WA	0.595 (7)	0.3816 (10)	0.329 (5)	0.056*
H5WB	0.675 (4)	0.4263 (19)	0.350 (5)	0.056*
O6W	0.8880 (4)	0.29373 (12)	0.7024 (3)	0.0326 (9)
H6WA	0.983 (4)	0.2883 (19)	0.752 (4)	0.049*
H6WB	0.821 (5)	0.2986 (19)	0.743 (4)	0.049*
N1	0.2806 (5)	0.73205 (14)	0.5353 (4)	0.0304 (10)
H1	0.327 (6)	0.7519 (13)	0.595 (3)	0.034 (16)*
N2	0.1923 (6)	0.74655 (15)	0.4409 (4)	0.0369 (11)
N3	0.1410 (5)	0.71110 (16)	0.3860 (4)	0.0343 (11)
N4	0.1933 (5)	0.67313 (14)	0.4425 (3)	0.0285 (10)
N6	0.3520 (7)	0.66094 (14)	0.6159 (5)	0.0359 (11)
H6E	0.350 (8)	0.6295 (9)	0.605 (6)	0.058 (17)*
H6F	0.428 (5)	0.6748 (17)	0.671 (3)	0.039 (16)*
C1A	0.8643 (6)	0.60517 (12)	0.6113 (5)	0.0175 (8)
C1B	0.3643 (7)	0.33185 (12)	0.6107 (5)	0.0199 (9)
C1C	0.1119 (6)	0.36424 (15)	0.3595 (4)	0.0168 (11)
C1D	0.6124 (6)	0.63694 (17)	0.3643 (4)	0.0184 (11)
C2A	0.7377 (5)	0.58230 (17)	0.6198 (4)	0.0183 (11)
H2A	0.653508	0.598172	0.625794	0.022*
C2B	0.4875 (6)	0.35437 (16)	0.5972 (4)	0.0188 (11)
H2B	0.570536	0.338353	0.589401	0.023*
C2C	−0.0109 (5)	0.38706 (17)	0.3733 (4)	0.0193 (11)
H2C	−0.093365	0.371084	0.382215	0.023*
C2D	0.7350 (5)	0.61467 (17)	0.3530 (4)	0.0184 (11)
H2D	0.819591	0.630798	0.348765	0.022*
C3A	0.7395 (5)	0.53613 (16)	0.6194 (4)	0.0187 (11)
C3B	0.4854 (6)	0.40080 (17)	0.5953 (4)	0.0192 (11)
C3C	−0.0100 (5)	0.43334 (18)	0.3737 (4)	0.0191 (11)
C3D	0.7329 (5)	0.56810 (18)	0.3479 (4)	0.0174 (11)
C4A	0.8617 (6)	0.51269 (12)	0.6098 (4)	0.0187 (8)
H4AA	0.860842	0.481011	0.608923	0.022*
C4B	0.3644 (6)	0.42429 (12)	0.6076 (5)	0.0187 (9)
H4BA	0.364279	0.455967	0.606989	0.022*
C4C	0.1111 (5)	0.45694 (17)	0.3617 (4)	0.0189 (11)
H4CA	0.111134	0.488618	0.362572	0.023*
C4D	0.6090 (6)	0.54441 (17)	0.3532 (4)	0.0193 (11)
H4DA	0.607574	0.512780	0.349269	0.023*
C5	0.2800 (6)	0.68670 (17)	0.5355 (4)	0.0273 (12)
C5A	0.9861 (5)	0.53605 (16)	0.6016 (4)	0.0181 (11)
C5B	0.2427 (6)	0.40082 (17)	0.6209 (4)	0.0187 (11)
C5C	0.2322 (5)	0.43368 (17)	0.3483 (4)	0.0173 (11)

C5D	0.4863 (5)	0.56776 (18)	0.3646 (4)	0.0216 (12)
C6A	0.9873 (6)	0.58229 (16)	0.6013 (4)	0.0165 (11)
H6A	1.071150	0.598085	0.594297	0.020*
C6B	0.2421 (6)	0.35474 (16)	0.6234 (4)	0.0205 (11)
H6B	0.159995	0.338982	0.633608	0.025*
C6C	0.2330 (5)	0.38723 (17)	0.3460 (4)	0.0209 (12)
H6C	0.314904	0.371532	0.335372	0.025*
C6D	0.4875 (5)	0.61409 (17)	0.3712 (4)	0.0182 (11)
H6D	0.404620	0.629780	0.380140	0.022*
C7A	0.8641 (7)	0.65467 (12)	0.6133 (5)	0.0184 (9)
C7B	0.3671 (7)	0.28226 (13)	0.6127 (5)	0.0226 (9)
C7C	0.1086 (6)	0.31442 (16)	0.3592 (4)	0.0221 (12)
C7D	0.6131 (6)	0.68655 (16)	0.3657 (4)	0.0201 (11)

Atomic displacement parameters (Å²)

	U^{11}	U^{22}	U^{33}	U^{12}	U^{13}	U^{23}
O1A	0.030 (2)	0.0114 (19)	0.058 (3)	−0.0034 (18)	0.0200 (19)	0.002 (2)
O1B	0.028 (2)	0.0120 (19)	0.071 (3)	−0.0023 (19)	0.015 (2)	0.002 (2)
O1C	0.029 (2)	0.012 (2)	0.056 (3)	0.0010 (17)	0.017 (2)	−0.0002 (19)
O1D	0.026 (2)	0.0123 (19)	0.065 (3)	0.0057 (17)	0.026 (2)	0.0000 (19)
O1W	0.027 (2)	0.0256 (18)	0.055 (3)	0.0030 (18)	0.016 (2)	0.0078 (18)
O2A	0.023 (2)	0.0164 (19)	0.046 (2)	−0.0011 (17)	0.0152 (18)	−0.0029 (19)
O2B	0.029 (2)	0.017 (2)	0.059 (3)	0.0029 (19)	0.017 (2)	0.002 (2)
O2C	0.027 (2)	0.0146 (19)	0.059 (3)	−0.0022 (18)	0.0166 (19)	0.0007 (19)
O2D	0.024 (2)	0.0159 (19)	0.055 (3)	0.0011 (17)	0.0213 (19)	0.0013 (19)
O2W	0.023 (2)	0.0281 (18)	0.041 (2)	0.0025 (17)	0.0116 (18)	0.0082 (17)
O3A	0.021 (2)	0.0172 (19)	0.051 (2)	−0.0030 (17)	0.0164 (18)	−0.0014 (19)
O3B	0.0203 (19)	0.0178 (19)	0.042 (2)	−0.0022 (16)	0.0153 (17)	0.0013 (17)
O3C	0.0168 (18)	0.0155 (19)	0.041 (2)	0.0044 (14)	0.0134 (16)	−0.0018 (17)
O3D	0.0187 (18)	0.0118 (18)	0.040 (2)	0.0003 (15)	0.0109 (16)	−0.0026 (15)
O3W	0.040 (2)	0.034 (2)	0.085 (4)	−0.0143 (19)	0.040 (2)	−0.027 (2)
O4A	0.0180 (19)	0.0153 (19)	0.053 (3)	0.0020 (16)	0.0172 (18)	−0.0008 (18)
O4B	0.0227 (19)	0.0179 (19)	0.039 (2)	0.0036 (16)	0.0133 (17)	0.0024 (17)
O4C	0.0186 (18)	0.0138 (18)	0.059 (3)	−0.0012 (15)	0.0176 (18)	−0.0030 (17)
O4D	0.023 (2)	0.0112 (18)	0.055 (3)	−0.0024 (15)	0.0185 (19)	−0.0017 (17)
O4W	0.040 (2)	0.032 (2)	0.045 (3)	0.0015 (19)	0.017 (2)	0.0029 (19)
O5W	0.024 (2)	0.029 (2)	0.063 (3)	−0.0006 (17)	0.017 (2)	−0.006 (2)
O6W	0.035 (2)	0.031 (2)	0.031 (2)	0.0020 (18)	0.0076 (17)	0.0004 (17)
N1	0.032 (3)	0.028 (2)	0.030 (3)	0.003 (2)	0.007 (2)	−0.003 (2)
N2	0.038 (3)	0.032 (3)	0.037 (3)	0.007 (2)	0.005 (2)	0.002 (2)
N3	0.036 (3)	0.034 (3)	0.033 (2)	−0.002 (2)	0.009 (2)	−0.005 (2)
N4	0.025 (2)	0.029 (2)	0.031 (3)	−0.0017 (19)	0.0075 (19)	−0.004 (2)
N6	0.040 (3)	0.026 (2)	0.035 (3)	−0.002 (3)	0.000 (2)	−0.002 (3)
C1A	0.020 (2)	0.0142 (18)	0.018 (2)	−0.001 (3)	0.0050 (17)	−0.002 (3)
C1B	0.020 (2)	0.0145 (19)	0.024 (2)	−0.001 (3)	0.0040 (18)	−0.001 (3)
C1C	0.019 (3)	0.007 (2)	0.024 (3)	0.002 (2)	0.005 (2)	0.000 (2)
C1D	0.020 (3)	0.015 (3)	0.019 (3)	0.002 (2)	0.003 (2)	0.000 (2)

C2A	0.013 (2)	0.021 (3)	0.022 (3)	0.000 (2)	0.005 (2)	0.000 (2)
C2B	0.015 (3)	0.014 (3)	0.027 (3)	0.002 (2)	0.005 (2)	−0.004 (2)
C2C	0.018 (3)	0.015 (3)	0.025 (3)	0.001 (2)	0.007 (2)	−0.001 (2)
C2D	0.017 (3)	0.012 (3)	0.027 (3)	−0.004 (2)	0.007 (2)	0.001 (2)
C3A	0.018 (3)	0.013 (2)	0.026 (3)	−0.004 (2)	0.006 (2)	0.001 (2)
C3B	0.015 (3)	0.018 (3)	0.024 (3)	−0.001 (2)	0.006 (2)	0.002 (2)
C3C	0.019 (3)	0.019 (3)	0.019 (3)	−0.001 (2)	0.005 (2)	0.002 (2)
C3D	0.015 (3)	0.017 (3)	0.022 (3)	0.004 (2)	0.008 (2)	−0.001 (2)
C4A	0.019 (2)	0.0118 (18)	0.025 (2)	0.002 (3)	0.0058 (17)	0.002 (3)
C4B	0.020 (2)	0.0096 (17)	0.027 (2)	−0.003 (2)	0.0072 (18)	0.002 (3)
C4C	0.023 (3)	0.010 (2)	0.025 (3)	0.003 (2)	0.009 (2)	−0.002 (2)
C4D	0.023 (3)	0.012 (2)	0.023 (3)	−0.001 (2)	0.007 (2)	−0.003 (2)
C5	0.026 (3)	0.029 (3)	0.031 (3)	−0.003 (2)	0.014 (2)	−0.002 (2)
C5A	0.015 (3)	0.018 (3)	0.022 (3)	0.002 (2)	0.005 (2)	−0.001 (2)
C5B	0.019 (3)	0.016 (3)	0.020 (3)	0.005 (2)	0.005 (2)	0.000 (2)
C5C	0.020 (3)	0.013 (3)	0.019 (3)	−0.001 (2)	0.007 (2)	0.000 (2)
C5D	0.018 (3)	0.017 (3)	0.029 (3)	−0.004 (2)	0.006 (2)	−0.002 (2)
C6A	0.017 (3)	0.012 (3)	0.022 (3)	0.000 (2)	0.007 (2)	0.001 (2)
C6B	0.020 (3)	0.017 (3)	0.024 (3)	−0.005 (2)	0.005 (2)	−0.003 (2)
C6C	0.020 (3)	0.014 (3)	0.031 (3)	0.001 (2)	0.010 (2)	0.001 (2)
C6D	0.017 (3)	0.016 (3)	0.022 (3)	0.002 (2)	0.006 (2)	−0.003 (2)
C7A	0.019 (2)	0.0138 (19)	0.023 (2)	0.001 (3)	0.0069 (17)	0.004 (3)
C7B	0.021 (2)	0.0155 (19)	0.032 (3)	−0.002 (3)	0.0083 (19)	−0.003 (3)
C7C	0.026 (3)	0.010 (2)	0.029 (3)	0.001 (2)	0.004 (2)	0.003 (2)
C7D	0.019 (3)	0.017 (3)	0.026 (3)	0.005 (2)	0.009 (2)	−0.001 (2)

Geometric parameters (Å, º)

O1A—H1A	0.99 (3)	N4—C5	1.332 (6)
O1A—C7A	1.302 (7)	N6—H6E	0.95 (3)
O1B—H1B	0.98 (3)	N6—H6F	0.96 (3)
O1B—C7B	1.315 (7)	N6—C5	1.332 (7)
O1C—H1C	0.98 (3)	C1A—C2A	1.412 (7)
O1C—C7C	1.316 (7)	C1A—C6A	1.388 (7)
O1D—H1D	0.96 (3)	C1A—C7A	1.485 (5)
O1D—C7D	1.301 (6)	C1B—C2B	1.401 (7)
O1W—H1WA	0.96 (3)	C1B—C6B	1.395 (7)
O1W—H1WB	0.95 (3)	C1B—C7B	1.487 (5)
O2A—C7A	1.247 (6)	C1C—C2C	1.404 (7)
O2B—C7B	1.232 (7)	C1C—C6C	1.390 (7)
O2C—C7C	1.227 (6)	C1C—C7C	1.494 (7)
O2D—C7D	1.249 (6)	C1D—C2D	1.381 (7)
O2W—H2WA	0.95 (3)	C1D—C6D	1.390 (7)
O2W—H2WB	0.97 (3)	C1D—C7D	1.488 (7)
O3A—H3A	0.99 (3)	C2A—H2A	0.9500
O3A—C3A	1.377 (6)	C2A—C3A	1.385 (7)
O3B—H3B	0.96 (3)	C2B—H2B	0.9500
O3B—C3B	1.372 (6)	C2B—C3B	1.393 (7)

O3C—H3C	0.95 (3)	C2C—H2C	0.9500
O3C—C3C	1.370 (6)	C2C—C3C	1.388 (7)
O3D—H3D	0.95 (3)	C2D—H2D	0.9500
O3D—C3D	1.374 (6)	C2D—C3D	1.398 (7)
O3W—H3WA	0.97 (3)	C3A—C4A	1.388 (7)
O3W—H3WB	0.95 (3)	C3B—C4B	1.392 (7)
O4A—H4A	0.95 (3)	C3C—C4C	1.392 (7)
O4A—C5A	1.375 (6)	C3D—C4D	1.389 (7)
O4B—H4B	0.98 (3)	C4A—H4AA	0.9500
O4B—C5B	1.377 (6)	C4A—C5A	1.400 (7)
O4C—H4C	0.95 (3)	C4B—H4BA	0.9500
O4C—C5C	1.377 (6)	C4B—C5B	1.402 (7)
O4D—H4D	0.93 (2)	C4C—H4CA	0.9500
O4D—C5D	1.373 (6)	C4C—C5C	1.394 (7)
O4W—H4WA	0.97 (3)	C4D—H4DA	0.9500
O4W—H4WB	0.94 (3)	C4D—C5D	1.398 (7)
O5W—H5WA	0.96 (3)	C5A—C6A	1.387 (7)
O5W—H5WB	0.95 (3)	C5B—C6B	1.382 (7)
O6W—H6WA	0.96 (3)	C5C—C6C	1.393 (7)
O6W—H6WB	0.96 (3)	C5D—C6D	1.392 (7)
N1—H1	0.98 (3)	C6A—H6A	0.9500
N1—N2	1.359 (6)	C6B—H6B	0.9500
N1—C5	1.360 (6)	C6C—H6C	0.9500
N2—N3	1.300 (6)	C6D—H6D	0.9500
N3—N4	1.374 (6)		

C7A—O1A—H1A	107 (4)	O3C—C3C—C2C	117.7 (4)
C7B—O1B—H1B	115 (5)	O3C—C3C—C4C	121.5 (5)
C7C—O1C—H1C	105 (4)	C2C—C3C—C4C	120.8 (5)
C7D—O1D—H1D	117 (3)	O3D—C3D—C2D	122.0 (5)
H1WA—O1W—H1WB	112 (5)	O3D—C3D—C4D	117.4 (5)
H2WA—O2W—H2WB	100 (5)	C4D—C3D—C2D	120.6 (5)
C3A—O3A—H3A	110 (4)	C3A—C4A—H4AA	120.2
C3B—O3B—H3B	111 (4)	C3A—C4A—C5A	119.5 (3)
C3C—O3C—H3C	113 (3)	C5A—C4A—H4AA	120.2
C3D—O3D—H3D	105 (4)	C3B—C4B—H4BA	120.3
H3WA—O3W—H3WB	109 (6)	C3B—C4B—C5B	119.4 (3)
C5A—O4A—H4A	108 (4)	C5B—C4B—H4BA	120.3
C5B—O4B—H4B	109 (4)	C3C—C4C—H4CA	120.3
C5C—O4C—H4C	105 (3)	C3C—C4C—C5C	119.4 (4)
C5D—O4D—H4D	110 (3)	C5C—C4C—H4CA	120.3
H4WA—O4W—H4WB	116 (4)	C3D—C4D—H4DA	120.5
H5WA—O5W—H5WB	106 (5)	C3D—C4D—C5D	119.1 (4)
H6WA—O6W—H6WB	107 (5)	C5D—C4D—H4DA	120.5
N2—N1—H1	124 (3)	N4—C5—N1	107.8 (5)
N2—N1—C5	108.7 (4)	N4—C5—N6	126.8 (5)
C5—N1—H1	127 (3)	N6—C5—N1	125.4 (5)
N3—N2—N1	106.5 (4)	O4A—C5A—C4A	117.2 (4)

N2—N3—N4	110.8 (4)	O4A—C5A—C6A	122.3 (5)
C5—N4—N3	106.2 (4)	C6A—C5A—C4A	120.6 (5)
H6E—N6—H6F	121 (6)	O4B—C5B—C4B	121.3 (4)
C5—N6—H6E	118 (4)	O4B—C5B—C6B	117.8 (5)
C5—N6—H6F	117 (3)	C6B—C5B—C4B	120.9 (5)
C2A—C1A—C7A	118.6 (5)	O4C—C5C—C4C	118.2 (4)
C6A—C1A—C2A	121.3 (4)	O4C—C5C—C6C	121.0 (5)
C6A—C1A—C7A	120.1 (5)	C6C—C5C—C4C	120.8 (5)
C2B—C1B—C7B	118.2 (5)	O4D—C5D—C4D	121.3 (5)
C6B—C1B—C2B	121.7 (3)	O4D—C5D—C6D	117.8 (5)
C6B—C1B—C7B	120.1 (5)	C6D—C5D—C4D	120.9 (5)
C2C—C1C—C7C	118.0 (5)	C1A—C6A—H6A	120.5
C6C—C1C—C2C	121.1 (4)	C5A—C6A—C1A	119.1 (5)
C6C—C1C—C7C	120.9 (5)	C5A—C6A—H6A	120.5
C2D—C1D—C6D	121.5 (4)	C1B—C6B—H6B	120.7
C2D—C1D—C7D	119.0 (4)	C5B—C6B—C1B	118.7 (5)
C6D—C1D—C7D	119.5 (5)	C5B—C6B—H6B	120.7
C1A—C2A—H2A	120.8	C1C—C6C—C5C	118.9 (5)
C3A—C2A—C1A	118.3 (5)	C1C—C6C—H6C	120.5
C3A—C2A—H2A	120.8	C5C—C6C—H6C	120.5
C1B—C2B—H2B	120.8	C1D—C6D—C5D	118.7 (5)
C3B—C2B—C1B	118.4 (5)	C1D—C6D—H6D	120.7
C3B—C2B—H2B	120.8	C5D—C6D—H6D	120.7
C1C—C2C—H2C	120.6	O1A—C7A—C1A	115.8 (5)
C3C—C2C—C1C	118.9 (5)	O2A—C7A—O1A	122.9 (4)
C3C—C2C—H2C	120.6	O2A—C7A—C1A	121.3 (5)
C1D—C2D—H2D	120.4	O1B—C7B—C1B	114.9 (5)
C1D—C2D—C3D	119.2 (5)	O2B—C7B—O1B	123.1 (4)
C3D—C2D—H2D	120.4	O2B—C7B—C1B	121.9 (5)
O3A—C3A—C2A	116.8 (5)	O1C—C7C—C1C	113.9 (5)
O3A—C3A—C4A	121.9 (4)	O2C—C7C—O1C	123.9 (5)
C2A—C3A—C4A	121.2 (5)	O2C—C7C—C1C	122.2 (5)
O3B—C3B—C2B	122.0 (5)	O1D—C7D—C1D	116.6 (5)
O3B—C3B—C4B	117.2 (4)	O2D—C7D—O1D	122.2 (5)
C4B—C3B—C2B	120.8 (5)	O2D—C7D—C1D	121.2 (5)

O3A—C3A—C4A—C5A	179.5 (4)	C2D—C1D—C7D—O2D	2.8 (8)
O3B—C3B—C4B—C5B	−179.7 (4)	C2D—C3D—C4D—C5D	−0.4 (8)
O3C—C3C—C4C—C5C	179.7 (4)	C3A—C4A—C5A—O4A	179.4 (4)
O3D—C3D—C4D—C5D	179.7 (4)	C3A—C4A—C5A—C6A	−1.0 (9)
O4A—C5A—C6A—C1A	−179.1 (4)	C3B—C4B—C5B—O4B	179.7 (4)
O4B—C5B—C6B—C1B	−179.9 (5)	C3B—C4B—C5B—C6B	0.9 (9)
O4C—C5C—C6C—C1C	178.9 (4)	C3C—C4C—C5C—O4C	−179.7 (4)
O4D—C5D—C6D—C1D	−178.9 (4)	C3C—C4C—C5C—C6C	0.5 (8)
N1—N2—N3—N4	0.3 (5)	C3D—C4D—C5D—O4D	179.6 (5)
N2—N1—C5—N4	0.4 (5)	C3D—C4D—C5D—C6D	−0.4 (8)
N2—N1—C5—N6	−178.6 (5)	C4A—C5A—C6A—C1A	1.2 (8)
N2—N3—N4—C5	0.0 (5)	C4B—C5B—C6B—C1B	−1.0 (9)

N3—N4—C5—N1	−0.2 (5)	C4C—C5C—C6C—C1C	−1.3 (8)
N3—N4—C5—N6	178.7 (6)	C4D—C5D—C6D—C1D	1.1 (8)
C1A—C2A—C3A—O3A	−179.5 (5)	C5—N1—N2—N3	−0.4 (5)
C1A—C2A—C3A—C4A	−0.5 (9)	C6A—C1A—C2A—C3A	0.8 (9)
C1B—C2B—C3B—O3B	179.6 (4)	C6A—C1A—C7A—O1A	2.4 (8)
C1B—C2B—C3B—C4B	0.6 (9)	C6A—C1A—C7A—O2A	−177.8 (5)
C1C—C2C—C3C—O3C	−179.9 (4)	C6B—C1B—C2B—C3B	−0.7 (9)
C1C—C2C—C3C—C4C	−0.6 (8)	C6B—C1B—C7B—O1B	8.8 (9)
C1D—C2D—C3D—O3D	−179.6 (4)	C6B—C1B—C7B—O2B	−171.4 (5)
C1D—C2D—C3D—C4D	0.5 (8)	C6C—C1C—C2C—C3C	−0.2 (7)
C2A—C1A—C6A—C5A	−1.1 (9)	C6C—C1C—C7C—O1C	6.0 (8)
C2A—C1A—C7A—O1A	−177.7 (5)	C6C—C1C—C7C—O2C	−174.6 (5)
C2A—C1A—C7A—O2A	2.1 (9)	C6D—C1D—C2D—C3D	0.3 (8)
C2A—C3A—C4A—C5A	0.6 (9)	C6D—C1D—C7D—O1D	3.8 (7)
C2B—C1B—C6B—C5B	0.9 (9)	C6D—C1D—C7D—O2D	−175.3 (5)
C2B—C1B—C7B—O1B	−172.0 (5)	C7A—C1A—C2A—C3A	−179.1 (5)
C2B—C1B—C7B—O2B	7.9 (9)	C7A—C1A—C6A—C5A	178.8 (5)
C2B—C3B—C4B—C5B	−0.7 (9)	C7B—C1B—C2B—C3B	−180.0 (5)
C2C—C1C—C6C—C5C	1.2 (8)	C7B—C1B—C6B—C5B	−179.8 (5)
C2C—C1C—C7C—O1C	−174.3 (5)	C7C—C1C—C2C—C3C	−179.9 (5)
C2C—C1C—C7C—O2C	5.1 (8)	C7C—C1C—C6C—C5C	−179.1 (5)
C2C—C3C—C4C—C5C	0.5 (8)	C7D—C1D—C2D—C3D	−177.7 (5)
C2D—C1D—C6D—C5D	−1.1 (8)	C7D—C1D—C6D—C5D	177.0 (5)
C2D—C1D—C7D—O1D	−178.2 (5)		

Hydrogen-bond geometry (Å, º)

D—H···*A*	*D*—H	H···*A*	*D*···*A*	*D*—H···*A*
O1*A*—H1*A*···O2*B*^{i}	0.99 (3)	1.64 (3)	2.617 (5)	168 (6)
O1*B*—H1*B*···O2*A*^{ii}	0.98 (3)	1.65 (3)	2.626 (5)	177 (7)
O1*C*—H1*C*···O2*D*^{ii}	0.98 (3)	1.68 (3)	2.631 (5)	163 (5)
O1*D*—H1*D*···O2*C*^{i}	0.96 (3)	1.69 (3)	2.630 (5)	165 (5)
O1*W*—H1*WA*···O6*W*	0.96 (3)	1.94 (3)	2.899 (5)	179 (5)
O1*W*—H1*WB*···O4*B*^{iii}	0.95 (3)	1.98 (3)	2.920 (5)	167 (5)
O2*W*—H2*WA*···O3*A*	0.95 (3)	1.93 (3)	2.865 (5)	166 (5)
O2*W*—H2*WB*···O4*D*	0.97 (3)	1.92 (3)	2.843 (5)	158 (5)
O3*A*—H3*A*···O3*B*	0.99 (3)	1.76 (3)	2.743 (5)	172 (7)
O3*B*—H3*B*···O1*W*	0.96 (3)	1.70 (3)	2.657 (5)	170 (6)
O3*C*—H3*C*···O3*D*^{iv}	0.95 (3)	1.80 (3)	2.750 (4)	175 (5)
O3*D*—H3*D*···O3*W*^{iii}	0.95 (3)	1.64 (3)	2.582 (5)	168 (6)
O3*W*—H3*WA*···N3	0.97 (3)	2.68 (3)	3.610 (6)	161 (6)
O3*W*—H3*WA*···N4	0.97 (3)	1.85 (3)	2.784 (6)	162 (6)
O3*W*—H3*WB*···O4*B*^{v}	0.95 (3)	2.21 (5)	2.998 (6)	140 (5)
O3*W*—H3*WB*···O4*D*	0.95 (3)	2.37 (6)	2.942 (5)	119 (5)
O4*A*—H4*A*···O2*W*^{iii}	0.95 (3)	1.76 (3)	2.690 (5)	166 (6)
O4*B*—H4*B*···O4*A*^{iv}	0.98 (3)	1.74 (3)	2.701 (5)	165 (6)
O4*C*—H4*C*···O5*W*	0.95 (3)	1.71 (3)	2.607 (5)	154 (5)
O4*D*—H4*D*···O4*C*	0.93 (2)	1.75 (3)	2.672 (4)	169 (4)

O4*W*—H4*WA*···N2^{vi}	0.97 (3)	2.01 (4)	2.918 (6)	156 (5)
O4*W*—H4*WB*···O2*A*^{v}	0.94 (3)	2.04 (3)	2.936 (6)	158 (5)
O5*W*—H5*WA*···O4*W*	0.96 (3)	1.85 (3)	2.773 (5)	162 (6)
O5*W*—H5*WB*···O3*C*^{iii}	0.95 (3)	1.95 (3)	2.901 (5)	172 (6)
O6*W*—H6*WA*···N3^{vii}	0.96 (3)	1.97 (3)	2.885 (6)	159 (5)
O6*W*—H6*WB*···O2*D*^{viii}	0.96 (3)	1.95 (3)	2.876 (5)	161 (5)
N1—H1···O6*W*^{ix}	0.98 (3)	1.86 (3)	2.837 (6)	172 (5)
N6—H6*E*···O2*W*	0.95 (3)	2.11 (3)	3.065 (5)	177 (6)
N6—H6*F*···O4*W*^{viii}	0.96 (3)	2.07 (3)	2.973 (7)	157 (5)

Symmetry codes: (i) *x*+1/2, *y*+1/2, *z*; (ii) *x*−1/2, *y*−1/2, *z*; (iii) *x*+1, *y*, *z*; (iv) *x*−1, *y*, *z*; (v) *x*, −*y*+1, *z*−1/2; (vi) *x*+1/2, *y*−1/2, *z*; (vii) *x*+1, −*y*+1, *z*+1/2; (viii) *x*, −*y*+1, *z*+1/2; (ix) *x*−1/2, *y*+1/2, *z*.

5-Aminotetrazolium 3,5-dinitrosalicylate (II)

Crystal data

$CH_4N_5^+·C_7H_3N_2O_7^-$
M_r = 313.21
Monoclinic, $P2_1/c$
a = 6.2591 (3) Å
b = 11.1312 (5) Å
c = 17.2257 (9) Å
β = 98.646 (5)°
V = 1186.50 (10) Å^3
Z = 4
F(000) = 640
D_x = 1.753 Mg m^{-3}
Cu *Kα* radiation, *λ* = 1.54184 Å
Cell parameters from 7845 reflections
θ = 6.5–68.1°
μ = 1.37 mm^{-1}
T = 173 K
Plate, yellow
0.07 × 0.03 × 0.01 mm

Data collection

Rigaku XtaLAB P100K diffractometer
Radiation source: Rotating Anode, Rigaku MM-007HF
Rigaku Osmic Confocal Optical System monochromator
ω and *φ* scans
Absorption correction: multi-scan (CrysAlis PRO; Rigaku OD, 2019)
T_{min} = 0.860, T_{max} = 1.000
4182 measured reflections
4182 independent reflections
3644 reflections with $I > 2\sigma(I)$
R_{int} = 0.041
θ_{max} = 68.3°, θ_{min} = 4.8°
h = −7→7
k = −13→13
l = −20→20

Refinement

Refinement on F^2
Least-squares matrix: full
$R[F^2 > 2\sigma(F^2)]$ = 0.041
$wR(F^2)$ = 0.114
S = 1.04
4182 reflections
221 parameters
6 restraints
Primary atom site location: dual
Hydrogen site location: mixed
H atoms treated by a mixture of independent and constrained refinement
$w = 1/[\sigma^2(F_o^2) + (0.0876P)^2 + 0.0468P]$ where $P = (F_o^2 + 2F_c^2)/3$
$(\Delta/\sigma)_{max}$ = 0.001
$\Delta\rho_{max}$ = 0.46 e Å^{-3}
$\Delta\rho_{min}$ = −0.43 e Å^{-3}
Extinction correction: SHELXL2018 (Sheldrick, 2015b), $Fc^*=kFc[1+0.001xFc^2\lambda^3/\sin(2\theta)]^{-1/4}$
Extinction coefficient: 0.015 (2)

Special details

Geometry. All e.s.d.'s (except the e.s.d. in the dihedral angle between two l.s. planes) are estimated using the full covariance matrix. The cell e.s.d.'s are taken into account individually in the estimation of e.s.d.'s in distances, angles and torsion angles; correlations between e.s.d.'s in cell parameters are only used when they are defined by crystal symmetry. An approximate (isotropic) treatment of cell e.s.d.'s is used for estimating e.s.d.'s involving l.s. planes.

Refinement. Refined as a 2-component twin.

Fractional atomic coordinates and isotropic or equivalent isotropic displacement parameters (Å²)

	x	*y*	*z*	U_{iso}*/U_{eq}
O1	0.2093 (3)	0.53433 (10)	0.31038 (7)	0.0508 (4)
O2	0.22700 (19)	0.40435 (9)	0.40980 (7)	0.0342 (3)
O3	0.3059 (3)	0.57855 (12)	0.68383 (7)	0.0507 (4)
O4	0.2069 (2)	0.76263 (12)	0.69133 (7)	0.0501 (4)
O5	0.2538 (3)	1.03140 (11)	0.47320 (8)	0.0549 (4)
O6	0.2542 (3)	0.95489 (11)	0.35884 (8)	0.0516 (4)
O7	0.24886 (18)	0.47913 (9)	0.54500 (6)	0.0317 (3)
H7	0.246 (4)	0.4277 (15)	0.4975 (8)	0.061 (7)*
N1	0.2817 (2)	0.18681 (13)	0.16865 (9)	0.0346 (3)
H1	0.299 (3)	0.1046 (13)	0.1548 (14)	0.055 (6)*
N2	0.2682 (2)	0.26852 (14)	0.10881 (9)	0.0388 (4)
N3	0.2448 (2)	0.37131 (13)	0.13805 (8)	0.0386 (4)
N4	0.2429 (2)	0.35865 (12)	0.21645 (8)	0.0341 (3)
H4	0.232 (3)	0.4274 (16)	0.2521 (12)	0.053 (6)*
N6	0.2792 (3)	0.19860 (13)	0.30761 (9)	0.0399 (4)
H6A	0.267 (3)	0.1158 (12)	0.3165 (12)	0.047 (6)*
H6B	0.254 (3)	0.2536 (15)	0.3472 (9)	0.034 (5)*
N12	0.2529 (2)	0.94559 (12)	0.42991 (9)	0.0344 (3)
N13	0.2538 (2)	0.67665 (12)	0.65356 (8)	0.0350 (4)
C5	0.2663 (3)	0.24353 (14)	0.23571 (10)	0.0304 (4)
C7	0.2489 (2)	0.59091 (13)	0.51941 (9)	0.0268 (3)
C8	0.2522 (2)	0.69166 (15)	0.56911 (9)	0.0293 (4)
C9	0.2516 (2)	0.80802 (14)	0.54100 (9)	0.0302 (4)
H9	0.252148	0.874795	0.575371	0.036*
C10	0.2504 (2)	0.82423 (13)	0.46158 (9)	0.0288 (4)
C11	0.2430 (2)	0.72878 (13)	0.40960 (9)	0.0281 (4)
H11	0.240017	0.742847	0.355051	0.034*
C12	0.2401 (2)	0.61341 (13)	0.43800 (9)	0.0267 (3)
C13	0.2250 (3)	0.51070 (14)	0.38150 (9)	0.0315 (4)

Atomic displacement parameters (Å²)

	U^{11}	U^{22}	U^{33}	U^{12}	U^{13}	U^{23}
O1	0.1058 (11)	0.0227 (6)	0.0250 (6)	0.0047 (6)	0.0131 (7)	−0.0003 (5)
O2	0.0542 (7)	0.0206 (6)	0.0285 (6)	0.0000 (4)	0.0088 (5)	0.0009 (4)
O3	0.0854 (10)	0.0397 (7)	0.0262 (7)	0.0010 (6)	0.0053 (6)	0.0057 (5)
O4	0.0807 (10)	0.0435 (8)	0.0294 (7)	0.0012 (6)	0.0184 (6)	−0.0085 (5)
O5	0.1030 (12)	0.0233 (7)	0.0395 (7)	−0.0016 (6)	0.0141 (7)	−0.0070 (5)

O6	0.1007 (11)	0.0271 (6)	0.0286 (7)	−0.0019 (6)	0.0145 (7)	0.0046 (5)
O7	0.0470 (7)	0.0233 (6)	0.0248 (6)	−0.0010 (4)	0.0056 (5)	0.0046 (4)
N1	0.0419 (7)	0.0285 (7)	0.0334 (7)	0.0007 (5)	0.0055 (6)	−0.0062 (6)
N2	0.0491 (8)	0.0383 (8)	0.0293 (8)	−0.0001 (6)	0.0066 (6)	−0.0064 (6)
N3	0.0536 (9)	0.0368 (8)	0.0254 (7)	−0.0006 (6)	0.0059 (6)	0.0001 (6)
N4	0.0538 (8)	0.0257 (7)	0.0232 (7)	−0.0002 (6)	0.0070 (6)	−0.0017 (5)
N6	0.0611 (9)	0.0242 (7)	0.0349 (8)	0.0003 (6)	0.0086 (7)	0.0033 (6)
N12	0.0500 (8)	0.0225 (7)	0.0303 (8)	−0.0012 (5)	0.0051 (6)	−0.0009 (5)
N13	0.0473 (8)	0.0349 (8)	0.0231 (7)	−0.0045 (6)	0.0065 (6)	−0.0026 (5)
C5	0.0349 (8)	0.0245 (7)	0.0316 (9)	−0.0019 (6)	0.0050 (6)	−0.0050 (6)
C7	0.0309 (7)	0.0246 (8)	0.0251 (8)	−0.0008 (5)	0.0046 (6)	0.0014 (6)
C8	0.0346 (8)	0.0312 (8)	0.0224 (7)	−0.0018 (6)	0.0050 (6)	−0.0015 (6)
C9	0.0370 (8)	0.0271 (8)	0.0265 (8)	−0.0012 (6)	0.0053 (6)	−0.0060 (6)
C10	0.0369 (8)	0.0218 (8)	0.0278 (8)	−0.0013 (5)	0.0057 (6)	0.0001 (6)
C11	0.0362 (8)	0.0245 (8)	0.0240 (8)	−0.0003 (6)	0.0061 (6)	−0.0003 (6)
C12	0.0332 (8)	0.0239 (8)	0.0233 (8)	0.0002 (5)	0.0053 (6)	0.0008 (6)
C13	0.0474 (9)	0.0231 (7)	0.0243 (8)	0.0005 (6)	0.0064 (7)	0.0003 (6)

Geometric parameters (Å, º)

O1—C13	1.242 (2)	N6—H6A	0.940 (13)
O2—C13	1.2796 (19)	N6—H6B	0.947 (12)
O3—N13	1.2327 (19)	N6—C5	1.327 (2)
O4—N13	1.2176 (19)	N12—C10	1.458 (2)
O5—N12	1.2113 (18)	N13—C8	1.463 (2)
O6—N12	1.230 (2)	C7—C8	1.409 (2)
O7—H7	0.997 (7)	C7—C12	1.417 (2)
O7—C7	1.3200 (18)	C8—C9	1.383 (2)
N1—H1	0.956 (13)	C9—H9	0.9500
N1—N2	1.368 (2)	C9—C10	1.379 (2)
N1—C5	1.333 (2)	C10—C11	1.386 (2)
N2—N3	1.267 (2)	C11—H11	0.9500
N3—N4	1.360 (2)	C11—C12	1.375 (2)
N4—H4	0.989 (12)	C12—C13	1.495 (2)
N4—C5	1.326 (2)		

C7—O7—H7	105.5 (12)	O7—C7—C8	123.23 (14)
N2—N1—H1	116.4 (15)	O7—C7—C12	119.67 (14)
C5—N1—H1	134.1 (15)	C8—C7—C12	117.09 (13)
C5—N1—N2	109.50 (14)	C7—C8—N13	120.70 (14)
N3—N2—N1	107.38 (13)	C9—C8—N13	117.05 (14)
N2—N3—N4	108.66 (14)	C9—C8—C7	122.25 (14)
N3—N4—H4	123.2 (14)	C8—C9—H9	121.0
C5—N4—N3	109.36 (13)	C10—C9—C8	118.00 (15)
C5—N4—H4	127.4 (14)	C10—C9—H9	121.0
H6A—N6—H6B	119.4 (18)	C9—C10—N12	119.59 (14)
C5—N6—H6A	121.8 (13)	C9—C10—C11	122.37 (14)
C5—N6—H6B	115.8 (12)	C11—C10—N12	118.03 (14)

O5—N12—O6	123.11 (14)	C10—C11—H11	120.4
O5—N12—C10	119.98 (14)	C12—C11—C10	119.14 (14)
O6—N12—C10	116.91 (13)	C12—C11—H11	120.4
O3—N13—C8	118.92 (14)	C7—C12—C13	119.89 (13)
O4—N13—O3	122.68 (15)	C11—C12—C7	121.08 (14)
O4—N13—C8	118.38 (14)	C11—C12—C13	119.03 (14)
N4—C5—N1	105.11 (15)	O1—C13—O2	124.49 (14)
N4—C5—N6	125.92 (15)	O1—C13—C12	117.90 (14)
N6—C5—N1	128.93 (16)	O2—C13—C12	117.60 (13)

O3—N13—C8—C7	17.9 (2)	N12—C10—C11—C12	−179.87 (14)
O3—N13—C8—C9	−162.77 (15)	N13—C8—C9—C10	179.93 (13)
O4—N13—C8—C7	−163.36 (16)	C5—N1—N2—N3	−0.14 (19)
O4—N13—C8—C9	16.0 (2)	C7—C8—C9—C10	−0.8 (2)
O5—N12—C10—C9	−0.8 (3)	C7—C12—C13—O1	177.30 (15)
O5—N12—C10—C11	178.14 (16)	C7—C12—C13—O2	−2.0 (2)
O6—N12—C10—C9	179.14 (15)	C8—C7—C12—C11	2.4 (2)
O6—N12—C10—C11	−1.9 (2)	C8—C7—C12—C13	−176.95 (14)
O7—C7—C8—N13	−0.6 (2)	C8—C9—C10—N12	−179.13 (14)
O7—C7—C8—C9	−179.84 (14)	C8—C9—C10—C11	2.0 (2)
O7—C7—C12—C11	−179.06 (14)	C9—C10—C11—C12	−1.0 (2)
O7—C7—C12—C13	1.6 (2)	C10—C11—C12—C7	−1.3 (2)
N1—N2—N3—N4	0.02 (19)	C10—C11—C12—C13	178.08 (14)
N2—N1—C5—N4	0.20 (18)	C11—C12—C13—O1	−2.1 (2)
N2—N1—C5—N6	−177.39 (16)	C11—C12—C13—O2	178.63 (15)
N2—N3—N4—C5	0.1 (2)	C12—C7—C8—N13	177.89 (13)
N3—N4—C5—N1	−0.19 (18)	C12—C7—C8—C9	−1.4 (2)
N3—N4—C5—N6	177.50 (16)		

Hydrogen-bond geometry (Å, º)

D—H···*A*	*D*—H	H···*A*	*D*···*A*	*D*—H···*A*
O7—H7···O2	1.00 (1)	1.52 (1)	2.4576 (15)	155 (2)
N1—H1···O3^{i}	0.96 (1)	2.10 (2)	2.967 (2)	150 (2)
N1—H1···O7^{i}	0.96 (1)	2.09 (2)	2.8033 (17)	130 (2)
N4—H4···O1	0.99 (1)	1.58 (1)	2.5668 (17)	178 (2)
N6—H6*A*···O6^{ii}	0.94 (1)	1.94 (1)	2.8643 (19)	167 (2)
N6—H6*B*···O2	0.95 (1)	2.02 (1)	2.9367 (19)	164 (2)

Symmetry codes: (i) *x*, −*y*+1/2, *z*−1/2; (ii) *x*, *y*−1, *z*.